UNIVERSITY OF ALBERTA
LIBRARY

## Regulations Regarding Theses and Dissertations

Typescript copies of theses and dissertations for Master's and Doctor's degrees deposited in the University of Alberta Library, as the official Copy of the Faculty of Graduate Studies, may be consulted in the Reference Reading Room only.

A second copy is on deposit in the Department under whose supervision the work was done. Some Departments are willing to loan their copy to libraries, through the inter-library loan service of the University of Alberta Library.

These theses and dissertations are to be used only with due regard to the rights of the author. Written permission of the author and of the Department must be obtained through the University of Alberta Library when extended passages are copied. When permission has been granted, acknowledgement must appear in the published work.

This thesis or dissertation has been used in accordance with the above regulations by the persons listed below. The borrowing library is obligated to secure the signature of each user.

Please sign below:

| Date | Signature | Institution |
|---|---|---|
| | | |
| | | |
| | | |
| | | |
| | | |
| | | |
| | | |
| | | |
| | | |
| | | |
| | | |
| | | |

# THE UNIVERSITY OF ALBERTA

# CORE AND FLUID ANALYSIS OF UNCONSOLIDATED CORE AND HEAVY CRUDE OIL

BY

S. M. KHANDWALA

A THESIS

SUBMITTED TO THE FACULTY OF GRADUATE STUDIES

IN PARTIAL FULFILMENT OF THE REQUIREMENTS FOR THE

DEGREE OF MASTER OF SCIENCE

IN

PETROLEUM ENGINEERING

FACULTY OF ENGINEERING

DEPARTMENT OF CHEMICAL AND PETROLEUM ENGINEERING

EDMONTON, ALBERTA

JULY, 1966

## ABSTRACT

Various rock and fluid properties were measured in the laboratory to study some of the basic characteristics of unconsolidated sand and heavy crude oil.

To determine permeability and effective porosity, core samples were packed in a manner so as to approximately simulate existing reservoir conditions. Samples of heavy crude oil and separator gas were recombined to determine viscosity and saturation pressures at reservoir conditions.

Results indicate that fairly accurate estimations of the absolute permeability of unconsolidated formations could be made from the core analysis. It was also observed that the permeability of unconsolidated sands depends to a great extent on their shale and clay content and does not vary appreciably with the arrangement and the degree of packing. The porosity values compared favourably with theoretical and other experimental results.

The rate of solution and separation of gas in heavy oil was found to be extremely slow. Time required to reach equilibrium for the solution of 30 cubic feet of gas was more then 90 days. The measured viscosity of dead crude oil and its comparison to various other experimental results

# Contact

indicate that there was no concrete relation between viscosity of lower API gravity oils and their densities. Viscosity measurements on the recombined samples shows that the viscosity of heavy oil decreases appreciably with an increase of gas in solution up to 30 cubic feet per barrel.

## ACKNOWLEDGEMENTS

The author wishes to express his sincere appreciation for the helpful guidance and encouragement of Dr. D.L. Flock, Professor, Department of Chemical and Petroleum Engineering, University of Alberta, under whose supervision this investigation was carried out.

Thanks are also expressed to the technical staff of the Chemical and Petroleum Engineering shop for their assistance in design and construction of the equipment.

In addition the financial assistance of Alberta Research Council is gratefully acknowledged.

# TABLE OF CONTENTS

# LIST OF FIGURES

# LIST OF TABLES

# INTRODUCTION

This research project was undertaken to determine the absolute permeability of unconsolidated sands in their native state and to measure the viscosity of heavy crude oil at reservoir conditions. Other basic rock and fluid properties, such as porosity, oil and water content of the cores and the saturation pressures for recombined samples of heavy crude oil were also determined using standard core and fluid analysis techniques. Attempts have also been made to correlate basic rock properties of the unconsolidated sand with various information available from electric logs.

Because of the importance to the petroleum industry of the characteristics of fluid flow through the producing sand, extensive research has been conducted along these lines, and the results of many techniques of evaluating permeability and porosity have been published. Numerous standard procedures for determining permeability of the consolidated porous media have been cited in literature (1,2,3,4,5,6,). Standard core analysis techniques for the measurement of permeability for consolidated sands were not applicable for unconsolidated sand systems. When the formation consists of unconsolidated sand,

the problem of primary importance and maximum difficulty is that of recovering a core at the surface in such a manner that the original packing was undisturbed. During coring of the unconsolidated formations the sand is normally disturbed. The main problem was the repacking of the sample to reproduce a native state condition. Equipment and procedures have been developed for the packing of the unconsolidated sand to reproduce the approximate natural state for the determination of porosity and permeability.

One of the most important characteristics controling the movement of oil through the reservoir is the viscosity. Viscosity of crude oil is dependent upon two main factors; reservoir temperature and the amount of solution gas. The former may be assumed constant throughout the production history of a field but the latter is changing as solution gas evolves from the oil. Rolling ball type viscometers have been used extensively in the past (7,8) to measure the viscosity of crude oil at reservoir conditions. This type of viscometer could not be employed if any water was present in the sample. Quite often the separation of formation water from viscous crude oil samples is difficult. For this work a Bendix type lab-viscometer was employed to measure the

viscosity of heavy crude oil samples with gas in solution varying from 5 to 50 cubic feet per stock tank barrel of oil at approximately 75° F. The Bendix lab-viscometer provided a continuous indication of viscosity of a liquid by measuring the viscous dampening of the liquid on a small vibrating reed element.

Two core samples, twenty-five feet and forty feet in length, and three and a half inches in diameter were obtained from the wells in the Aberfeldy and Lone Rock Pools, respectively. The cores were cut using conventional rubber sleeve coring techniques and were sealed to avoid weathering and evaporation of fluid content. These core samples varied in lithology from unconsolidated, semiconsolidated and consolidated silty sand to hard and soft shale throughout their length. A representative sample from every one foot interval was analyzed for horizontal liquid permeability, effective porosity and oil and water content. Samples of dead crude oil and solution gas from a separator were recombined in the laboratory. Six samples varying from five to fifty cubic feet of gas per stock tank barrel of oil were analyzed for saturation pressures. Due to a considerable length of time involved in combining and separating gas from crude oil it was not possible to measure various other fluid properties.

Quantitative methods for determining the connate water content of sand have been developed. Unfortunately in the routine coring of oil formations, cores are contaminated with fresh water. The determination of the extent of such contamination is impractical. It was therefore desirable to establish the reservoir fluid content from the quantitative interpretation of electric logs using various established correlations. On the other hand attempts to determine the permeability of reservoir rock from the quantitative interpretation of logs have been unsuccessful. Therefore, the importance of permeability determination from core analyses has long been realized in the petroleum industry.

## REVIEW OF ELECTRIC LOG ANALYSIS

Electrical logging (9) is the measurement of the spontaneous potentials generated in the bore holes and the resistivities of the subsurface formations. The spontaneous or self potential log is a record of naturally occurring potential differences, between a surface electrode and an electrode in the column of conductive mud as the latter electrode is pulled up the wellbore past different formations. These potentials are recorded on the electrical log in millivolts. The variation in potential differences which are recorded on the SP log, are due to variations in potential of the downhole electrode, since the surface electrode is at some constant potential. These downhole potential variations are caused by the ohmic differences of potential in the mud column due to currents flowing around the intersection of the permeable bed, the adjacent shales, and the mud column. The currents, in turn, are driven essentially by electromotive forces, of electrochemical origin, which occur at the contacts between the drilling mud and the formation beds, and across adjacent shales.

Resistivity logging on the other hand consists of the measurement of the resistivities of formation, in situ,

by means of appropriate exploring devices lowered in the bore hole. In this process, the exploring device generally comprises three or more electrodes, kept at fixed distances from one another. An electrical current is caused to flow between two of the electrodes and others are used for measuring the potential differences created by the passage of current through the formations. The drilling mud, usually made with a water base, ensures electrical contact between the electrode and the formation. The potential differences, in turn, are a function of the resistivity of the medium in the neighbourhood of the electrode arrangement. The resistivity value is computed according to Ohm's law.

Normally two different types of resistivity curves, "Normal" and "Lateral" are recorded. The normal utilizes a single measuring electrode which measures the potential created by the current electrodes some distance apart in this bore hole. In the lateral device, potential differences between two measuring electrodes are measured. The potential is again created by current electrodes some distances apart in the bore hole. Several electrode spacings for the normal and lateral devices are usually run in the bore hole to vary the effective depth of investigation. When an examination is made of an electrical log, it will be noticed that the resistivity

values recorded at a given depth in a well may be different from one curve to the next. The reason for this is that the measurement does not deal with a single uniform and infinite medium, but rather with a series of zones, each of definite dimensions and each having its own resistivity.

The electrical log has been used extensively in a qualitative way to correlate formations penetrated by the drill in the exploitation of oil and gas reservoirs and to provide some indication of reservoir content. Numerous correlations (10, 11) have been established to predict the porosity, gas, oil, and water saturation and, in some cases, permeability of the consolidated formations from the electrical logs. Attempts were made here to establish similar types of correlations for unconsolidated sand with the help of the core analysis and electrical logs obtained on the same formation.

Dry rocks, with a few exceptions, are very good insulators. Perfectly dry rocks are seldom encountered in drilling. Therefore, subsurface formations have finite measurable resistivities because of the mineralized water which is contained in their pores or adsorbed on their interstitial clay. The resistivity of a formation is dependent largely upon the resistivity of the water present in that formation, the amount of such water present and the arrangement

of the water channels.

The ratio of the resistivity of a rock completely saturated with water, Ro, to the resistivity of water, Rw, is termed as formations resistivity factor (12), F, commonly known as formation factor.

$$F = \frac{Ro}{Rw} \text{ ----------(1)}$$

The formation factor depends on the structure of the formations. Literally thousands of laboratory determinations have been made of thousands of consolidated samples, and it has been found that the resistivity factor of a clean formation can be related to its porosity by a simple emperical formula of the form

$$F = \frac{a}{\emptyset^m} \text{ ----------(2)}$$

where a and m are two constants.

F = Formation resistivity factor

$\emptyset$ = Porosity in fraction

From the results of numerous observations the relation between formation resistivities and water saturation can be expressed by the following emperical equation.

$$Sw = (Ro/Rt)^{1/n} \text{ ----------(3)}$$

where

$R_t$ = Resistivity of the formation (containing hydrocarbons and formation water), true resistivity.

Ro = Resistivity of the same formation when entirely saturated with water.

Sw = Water saturation of this formation.

n = Constant

In the equation (3) Ro may be replaced by its equivalent, F x Rw from equation (2) and then it may be written

$$Sw = (Ro/R_t)^{1/n} = (F \times Rw/R_t)^{1/n} \text{ --------(4)}$$

For clean unconsolidated sand and for consolidated sand the value of n appears to be close to 2.0. This has been established by a number of experimental results both on the unconsolidated and the consolidated sand. Thus, an approximate relation can be written.

$$Sw = \sqrt{\frac{Ro}{R_t}} \text{ ----------(5)}$$

or

$$Sw = \sqrt{\frac{F \times Rw}{R}} \text{ ----------(6)}$$

A number of correlations of the type shown in equation (7) has been derived for consolidated sand from electric logs for the quantitative interpretation of permeability. Data obtained from various sources have given different values for a and e.

$$F \times \emptyset = a.\ K^{-e} \text{----------(7)}$$

where

F = formation factor

$\emptyset$ = fractional porosity

K = permeability in md.

The correlation of the type shown above gives only an approximate evaluation of permeability especially in view of the fact that the permeability curve versus $F \times \emptyset$ is very steep and a small variation in the $F \times \emptyset$ value results in an appreciable variation in K. At best it can only be hoped that the relation gives an idea of the order of magnitude of permeability.

Another approach to permeability determination from electric logs may be had from observing that above the transition zone (i.e. in the irreducible water-saturation zone) the prevailing water saturation is a function of both porosity and permeability through the empirical relation

$$K = 250\ \frac{\emptyset 3}{Swir}$$

where

Swir = irreducible water saturation.

The primary disadvantage of this type of correlation is the determination of irreducible water saturation. Should the water saturation value so obtained be different from the

irreducible value, the determined permeability by the above expression would naturally be erroneous.

# EXPERIMENTAL EQUIPMENT AND PROCEDURE

## PACKING OF UNCONSOLIDATED SAND

A representative sample of the unconsolidated core in its natural form from every one foot interval was packed in a lucite container of cylindrical shape. The cylinder was two and a half inches in length with an internal diameter of one inch and an external diameter of one and a half inches. A solid rod of lucite with a diameter slightly less than the internal diameter of the cylinder was utilized for tamping the sand. The cylinder was filled with sand with little disturbance of the original arrangement of sand and shale particles. This was accomplished by obtaining a plug of sand more than an inch in diameter and packed in such a manner so as to represent the horizontal direction to flow. The mud cake formed around the core due to mud filtration was carefully scraped off the sand. The ends of the cylinder were sealed with quarter inch thick lucite plate using ethylene dichloride as a glue.

The lucite cylinder was then transferred into a high pressure and high temperature chamber as shown in Figure 1. An electronic relay was used to control the temperature of the oil bath and nitrogen was utilized to

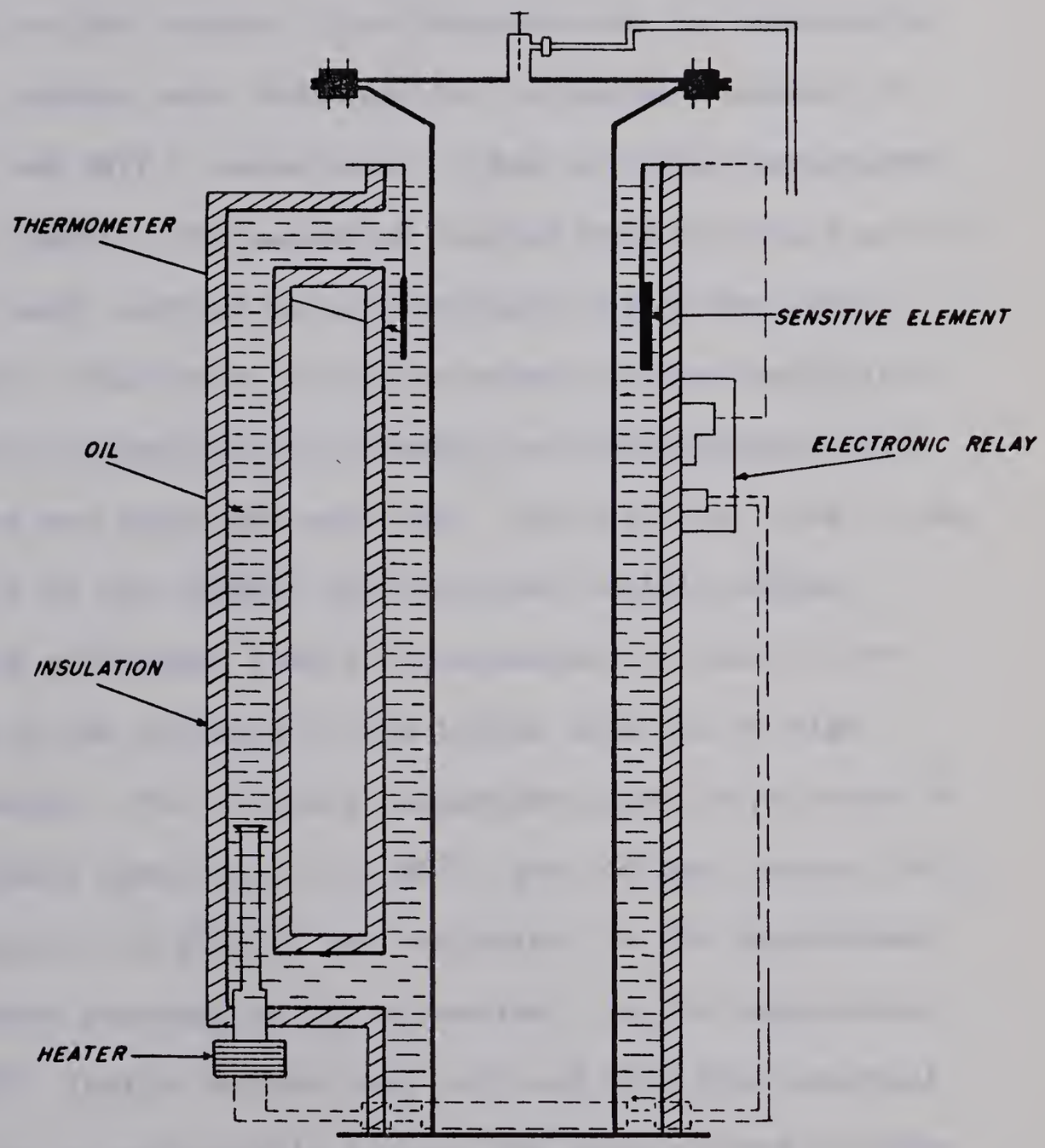


FIGURE NO. 1

SCHEMATIC DIAGRAM OF HIGH PRESSURE AND HIGH TEMPERATURE CHAMBER

pressurize the chamber. The pressure and the temperature of the chamber were increased in a stepwise increment of 50 psi and 30°F., respectively. Due to higher temperature in the chamber, the gas which evolved from the residual oil in the sand, exerted certain pressure inside the lucite cylinder. Therefore, it was necessary to have sufficient pressure initially in the chamber to counterbalance this pressure and avoid any explosion. On the other hand if the pressure in the chamber was increased rapidly without allowing sufficient time for temperature to rise, it resulted in the cracking of the lucite caps due to high compression. The ultimate temperature and the pressure in the chamber were raised to 260°F. and 650 psi, respectively. The pressure of 650 psi was equivalent to the approximate overburden pressure in the formation. At the temperature of 260°F. lucite becomes very soft and with high external pressure it was possible to seal the sides of the cylinder and obtain more compact packing. The cylinders were left in the chamber for approximately 48 hours after which the temperature of the chamber was reduced to room temperature and the pressure released by bleeding off the nitrogen gas.

The end caps of the cylinders were then machined carefully on the lath with little disturbance of the packing.

The cylinder with two open ends was then mounted between the end plates made of brass and held together with tie rods. The unit was used as a core holder. A hole bored in the middle of brass plates and tapped to hold a pressure tight fitting served for injecting fluid at one end and producing at the other. The pressure seal at each end was obtained with a neoprene-o-ring between the plates and the cylinder.

## POROSITY AND PERMEABILITY DETERMINATION

The core holder was mounted in the porosity and permeability apparatus as shown in Figure 2. To obtain the absolute permeability and true effective porosity it was necessary to clean the core and remove all the residual fluid. This was accomplished by flushing pentane through the core until all the residual oil in the sand had been dissolved and pure pentane was obtained at the downstream end. This was followed by air to remove pentane and to dry the core. Pentane was flushed again at a low upstream pressure to make sure all the residual oil had been removed and the sand was completely free of any oil stains. Clean and dry air, obtained by passing it through the air-trap and air-filter, was allowed to flow through the core for approximately four hours at a reasonably high up-stream pressure to dry the sand.

To avoid any possible swelling of the shale and clay particles present in sand or any other probable chemical reactions due to the use of foreign liquid, it was deemed necessary to utilize either the formation water or artificial brine with similar salt content. It was not possible to obtain enough formation water for the experiment but the salt content was determined from the water analysis study

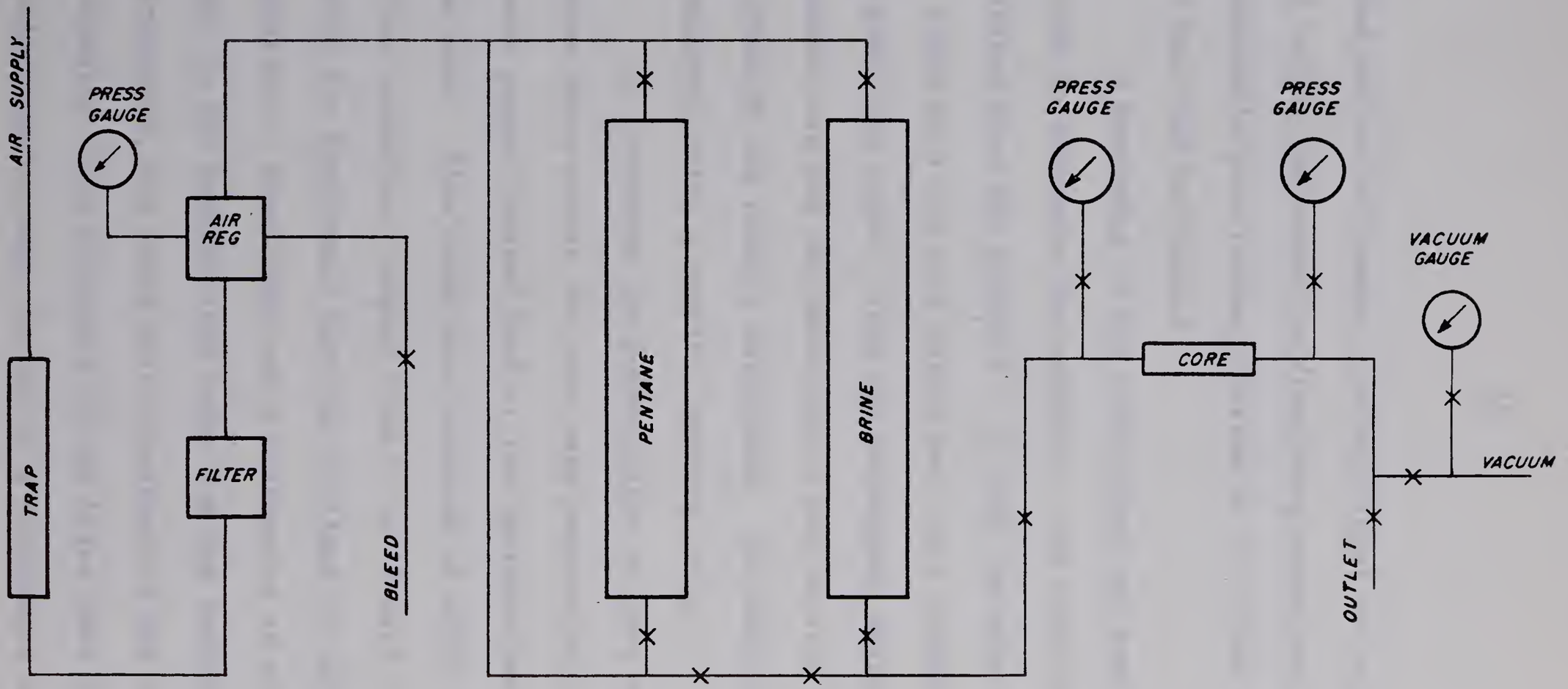


FIGURE NO. 2

SCHEMATIC DIAGRAM OF POROSITY AND PERMEABILITY APPARATUS

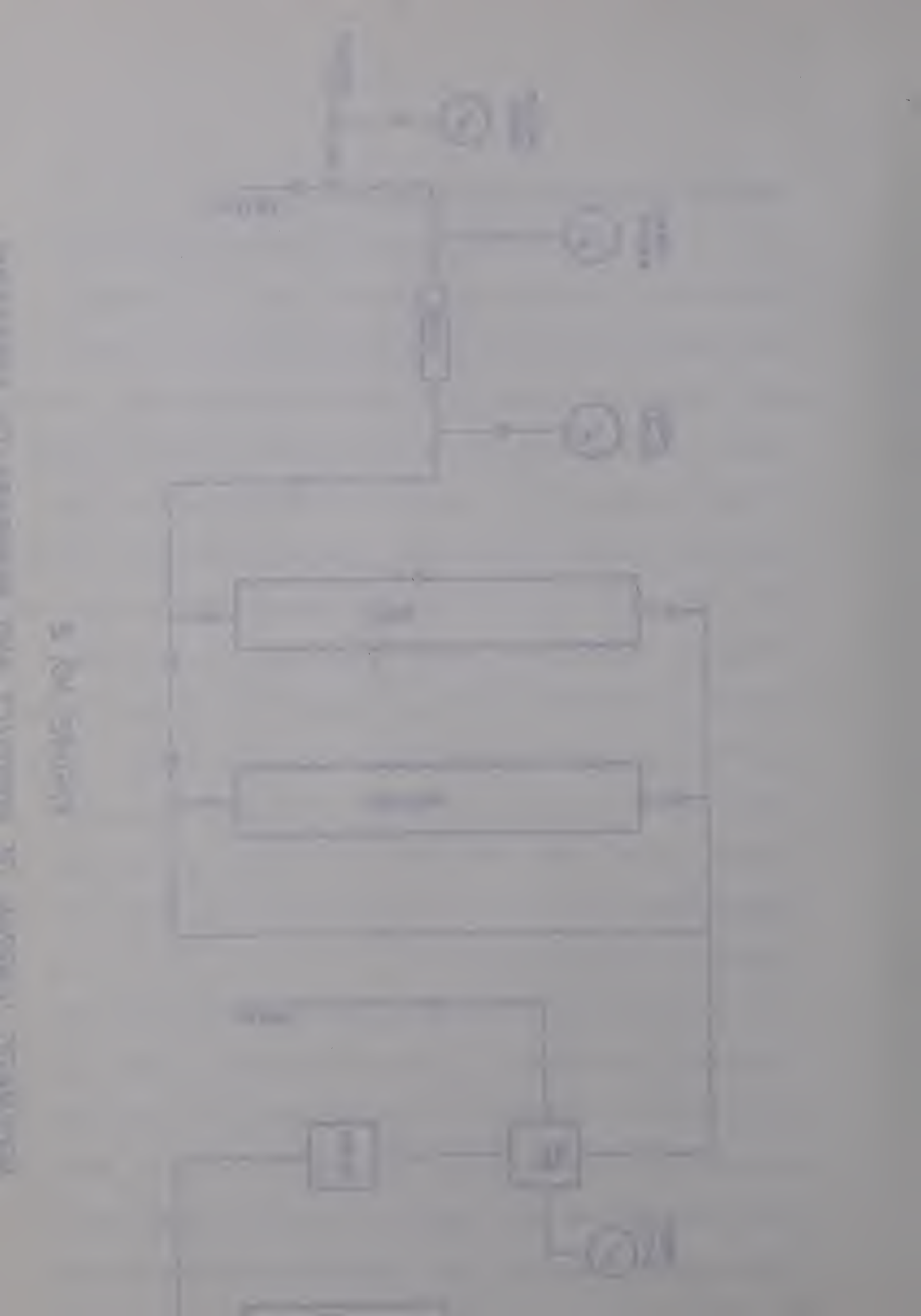

carried out on this water. An artificial brine was prepared in the laboratory by dissolving equivalent amounts of chemically pure sodium chloride in distilled water. The brine was then de-areated.

A knowledge of the bulk volume and pore volume was required to determine the porosity. The bulk volume was calculated from the geometry. To find the pore volume, the core along with the core holder was first weighed dry, then saturated with brine. From the subsequent weighing of the saturated core and the knowledge of the density of brine, the porosity was readily calculated. The density of brine was measured using a specific gravity scale.

To determine the permeability of core samples, pressure drops across the core were measured with precision pressure gauges located both at the upstream and the downstream ends. Flow rates were measured at eight different upstream pressures, ranging from 10 to 80 psig. Darcy's equation for horizontal flow was utilized to calculate the permeability. When there was a difference of more than two percent in the permeability value for the readings at different pressures, the cores were re-evacuated and the experiment was repeated. The viscosity of the brine used in the tests was determined through the use of a calibrated Ostwald-Fueske

type viscometer. The viscosity readings obtained in this manner were very close to one and were employed in the equation for calculating permeability.

RECOMBINATION OF OIL AND GAS SAMPLE.

A special apparatus was designed and constructed to study fluid properties of more than one sample at a time. Figure 3 shows a schematic diagram of this apparatus. It consisted of six stainless steel sample bottles utilized to store various recombined samples, two large bombs which contained dead crude oil and raw separator gas, a PVT cell employed to determine bubble point pressure of the recombined sample and a gas-oil separator to measure gas and oil formation volume factors. All the pumps shown in the diagram are volumetric displacement pumps with capacity of 500 milliliters each. The apparatus was equipped with three precision Heise gauges to provide various pressure readings.

Because of the excessive time required to reach equilibrium it was necessary to recombine more than one oil and gas sample at a time and store them in sample bottles. For example, the time required to obtain a sample with 30 standard cubic feet of gas in solution per stock tank barrel of oil was approximately 90 days. To obtain these recombined samples, the sample bottles were first evacuated and completely filled with mercury. The volume of mercury pumped into each of the bottles was measured and recorded. Two hundred

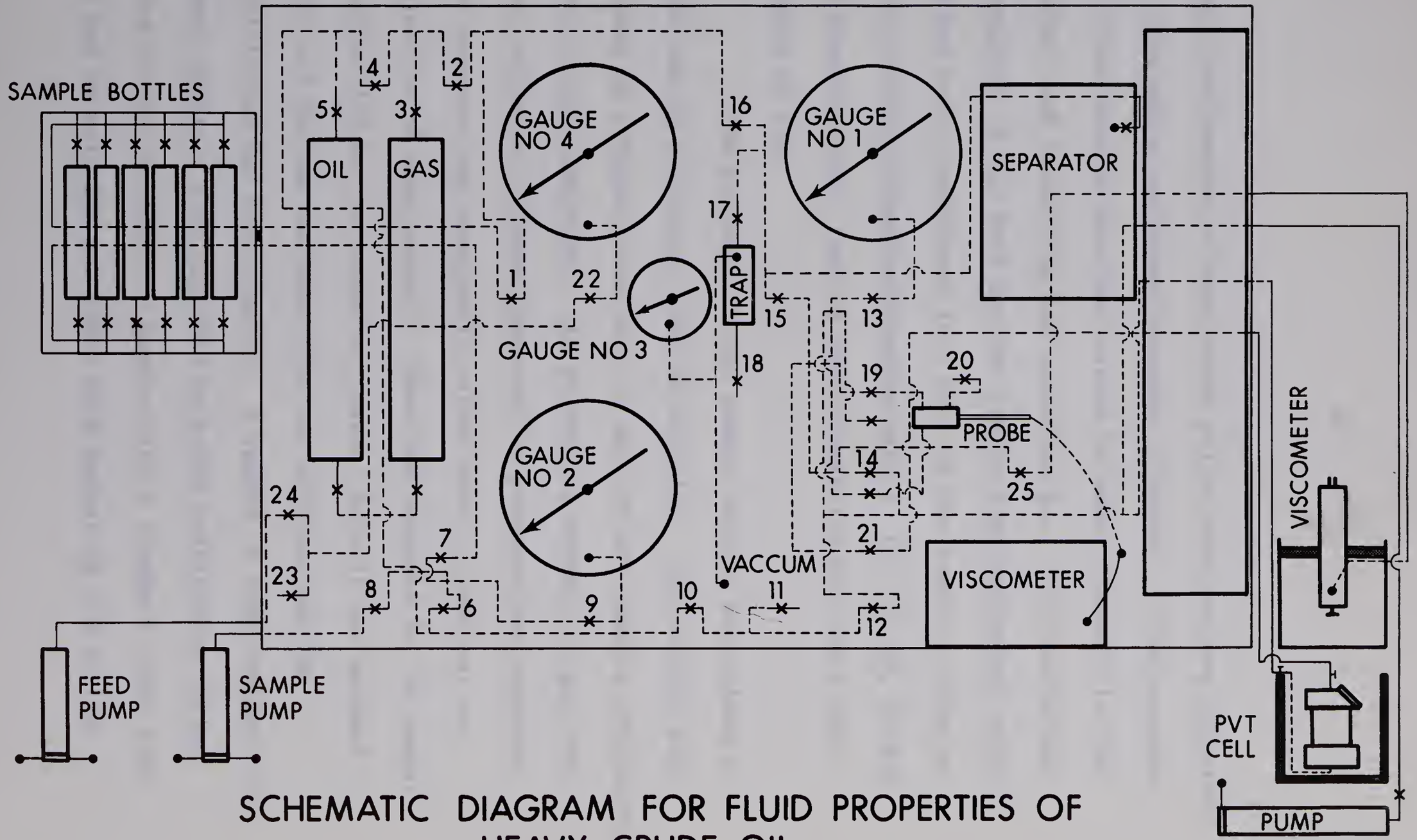


SCHEMATIC DIAGRAM FOR FLUID PROPERTIES OF HEAVY CRUDE OIL

FIG. 3

PNEUMATIC DIAGRAM FOR SAND MACHINE 04

cubic centimeters of dead crude oil at zero psi was injected by displacing equivalent amounts of mercury. The pressure in these bottles was then raised to equal pressure in the larger bomb containing raw separator gas. By simultaneous operation of the feed and the sample pump equivalent amounts of gas were transferred into each of the sample bottles so as to obtain recombined samples with 5, 10, 15, 25, 30 and 50 standard cubic feet of gas in solution per stock tank barrel of oil.

The pressure in the sample bottles was raised to 2000 psi to accelerate rate of solution. The bottles were rocked at constant intervals to agitate the samples and hasten equilibrium conditions. As increasing amounts of gas went into solution a gradual decrease in pressure was recorded. The pressure was constantly raised back to 2000 psi by injection of more mercury. When the pressure in the sample bottles did not decrease for several days it was assumed that all the gas had gone into the solution and the equilibrium had been reached. A record of time was kept for every sample. Time required to reach equilibrium varied from 25 days to obtain a sample with 5 standard cubic feet of gas in solution per stock tank barrel of oil to 120

days to obtain a sample with 50 standard cubic feet of gas in solution per stock tank barrel of oil.

## DETERMINATION OF SATURATION PRESSURE

For determination of the saturation pressure of each of the recombined samples one sample at a time was transferred into the PVT cell and pressure volume readings were taken at constant temperature. This was achieved by decreasing the cell pressure at constant interval and recording the simultaneous increase in volume. The bubble point at reservoir temperature was determined in the liquid phase cell by observing the first appearance of the gas bubble through the cell window. The pressure was reduced slowly at 50 psi intervals and agitated vigorously to insure equilibrium conditions. It is important to mention that when pressure was reduced below the bubble point it required several days of vigorous agitation to achieve equilibrium.

DETERMINATION OF VISCOSITY

The apparatus for viscosity determination of the recombined samples consist of a Bendix type lab-viscometer and a high pressure stainless steel cell. Figure 4 illustrates a cross-section through center of this cell. Rolling Ball type viscometer was also employed but due to the presence of free water in the sample it gave erroneous results. These two viscometers were connected to the apparatus for fluid properties and are shown in Figure 3.

The Bendix lab-viscometer provides a continuous indication of viscosity of a liquid by measuring the viscous dampening of the liquid on a small vibrating reed element. The probe which is connected to the main body of the viscometer via an electric cable has at its tip a thin blade approximately two inches long and quarter of an inch wide constructed from identical pieces of stainless steel and the magnetostrictive metal permadur. Its natural frequency of oscillation was 28,000 cycles per second. The probe blade was soldered to a diaphragm exactly at the blade's centre weld. The diaphragm forms the end surface of the cylindrical probe sleeve and the whole assembly comprised the replaceable probe tip. The probe coil at the right

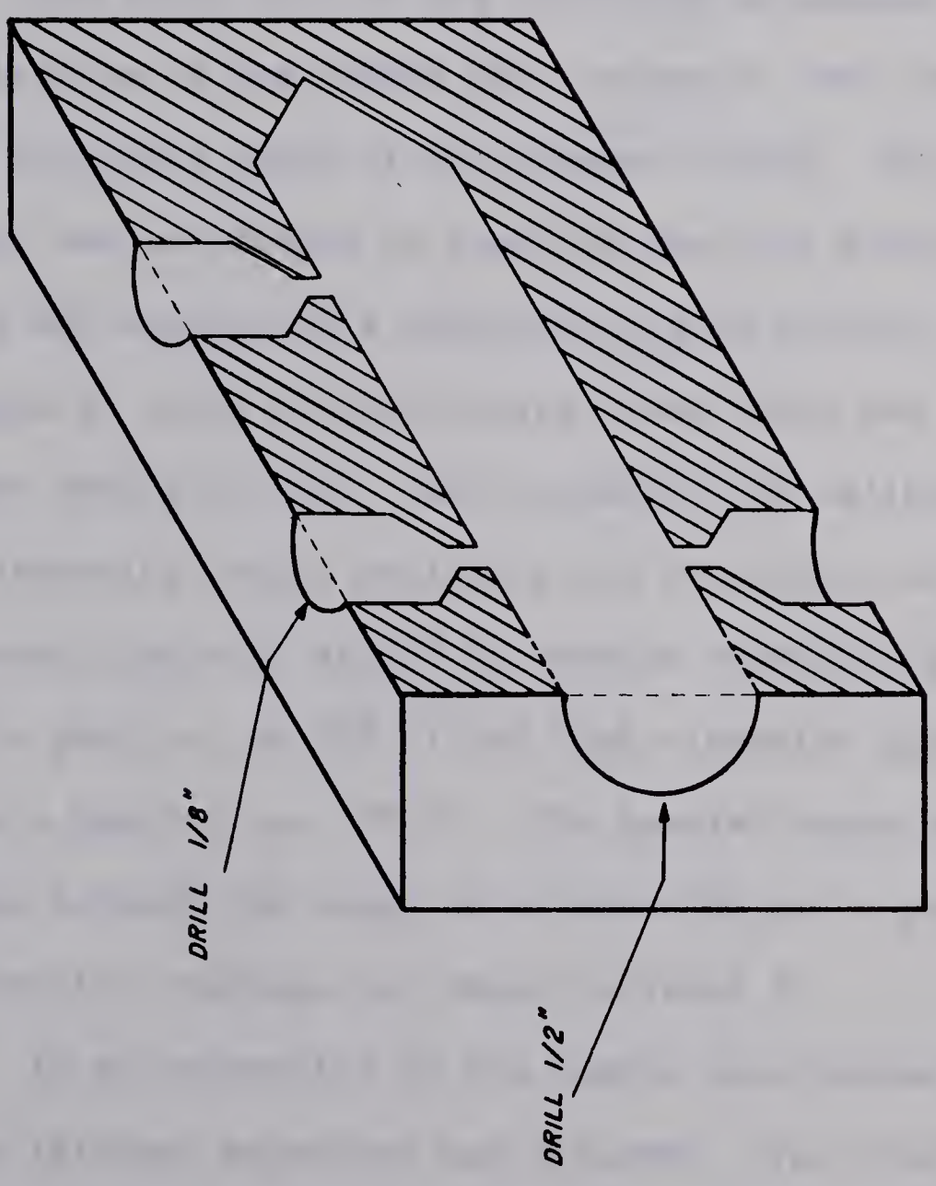


FIGURE NO. 4

CROSS-SECTION OF VISCOSITY CELL

hand end of the probe body slips into the sleeve and around the magnetostrictive half of the blade. The tip is held securely in place by a special lock-nut. A schematic diagram of the probe along with its blade is shown in Figure 5.

The first step in the viscosity determination was the calibration of the Bendix lab-viscometer over the expected viscosity range of the unknown fluids. The viscometer was calibrated to read the absolute product of viscosity and density of a newtonian liquid directly on the meter scale in units of centipoises times grams per cubic centimeter from 0-50,000. The viscometer was calibrated for two viscosity ranges employing low viscosity calibration oil (65 cps x gms/c.c. at 75° F), medium viscosity W30 oil (525 cps x gms/c.c. at 75° F) and high viscosity glycrene (1150 cps x gms/c.c. at 75° F). The Special Range was calibrated between the range of 65 and 1150 cps x gms/c.c. The calibration readings are shown in Tabel 8.

In the operation of the Bendix lab-viscometer a carefully laid-out procedure was followed. The viscometer was very sensitive and any small mistake resulted in completely erroneous readings. The following procedure for viscosity measurements in the laboratory was adopted step by step.

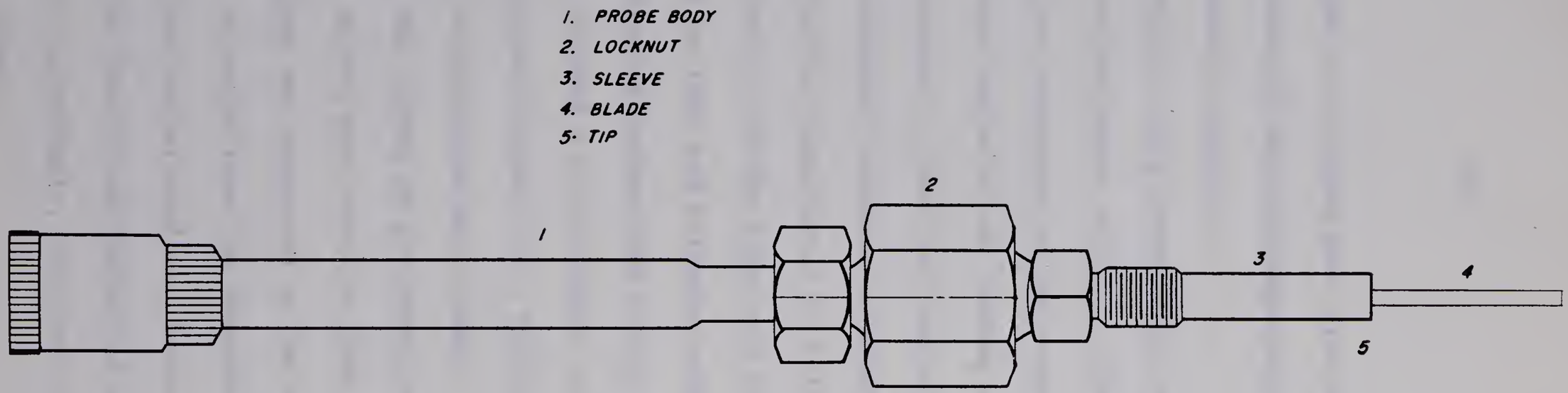


FIGURE NO. 5

SCHEMATIC DIAGRAM OF BENDIX-LAB VISCOMETER PROBE WITH REPLACEABLE TIP LOCKNUT

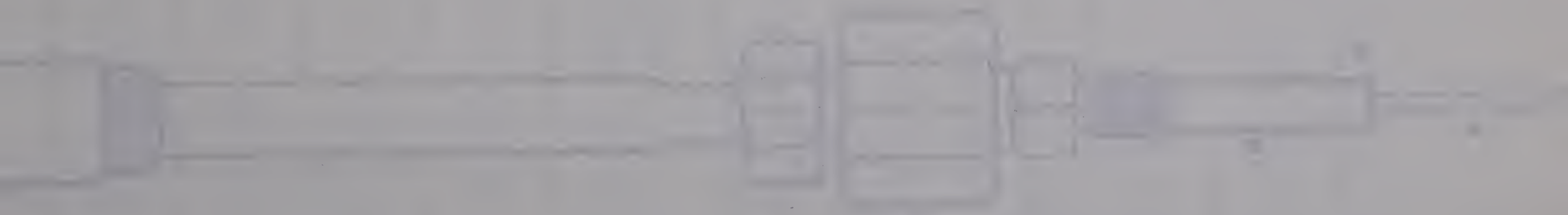

(1) The computer was located away from drafts and an area where the ambient temperature conditions were reasonably constant.

(2) Before connection the power switch was in the OFF position and the meter switch in ZERO position.

(3) The probe was connected to the computer with the furnished cable before turning on the power.

(4) It was important to see that the probe blade was free of mechanical stresses to afford stability and reproducible operation. To relieve the stresses the top of the blade was defected about quarter of an inch and released several times. The mechanical stresses were set up each time the blade touched a solid object or the power to the computer was turned off. Flicking of the blade was accomplished as follows:

   (a) Power was turned ON for about one minute.

   (b) Range switch was turned to ZERO position.

   (c) The blade was supported in the direction in which it would later be immersed or installed.

   (d) The blade was allowed to vibrate freely in air, and then the top was deflected quarter of an inch and let go suddenly. This was repeated two or three times.

(5) The probe blade was thoroughly cleaned with solvent and dried before being immersed in the sample as it measures only the layer in direct contact with the blade. The blade and at least one quarter inch of the probe was immersed. The cleaning was accomplished as follows:

(a) Range switch was set at "ZERO".

(b) Probe was immersed in suitable solvent.

(c) The probe was wiped clean with soft cloth, starting at the diaphragm and working toward the tip of the blade.

(6) The Bendix lab-viscometer computer required a warm-up period. The time required was about thirty minutes, depending on the initial temperature of the chasis and the surrounding air.

(7) The viscosity sensing element was operational at pressures from vacuum to 1,000 psig. and temperature as high as 650° F.

COMPUTER CALIBRATION

There was some electrical interaction between the zero and calibration controls. The calibration was repeated several times, when necessary, until the meter reading was correct at two points. Two media, with known viscosity-density

products at the calibration temperature were employed to provide these two points. The calibration was accomplished in a step wise manner as follows:

(a) Probe was inserted in low viscosity liquid. With zero control, the meter was made to read the proper viscosity.

(b) Probe was cleaned thoroughly.

(c) Probe was inserted in high viscosity liquid. With calibration control, the meter was made to read correct viscosity.

(d) Probe was cleaned thoroughly.

(e) Steps (a) and (b) were repeated.

(f) Steps (c) and (d) were repeated.

(g) Steps (e) and (f) were repeated until correct at both points.

For determination of viscosities of the recombined samples the viscosity cell and the probe were connected with rest of the apparatus as shown in figure 3. The cell was evacuated for several hours until a vacuum of one millimeter of mercury was obtained. It was then filled with mercury from bottom and pressurized to 500 psig. (above saturation pressure of the samples). A sample was pumped in the cell from top and by simultaneous use of two pumps the sample

was transferred into the cell without reducing the pressure below the saturation pressure. Care was taken not to exceed the pressure above 1,000 psi, so as not to damage the probe. The readings were repeated several times until three consecutive duplications in the readings were obtained.

# RESULTS AND DISCUSSION

## CORE PROPERTIES

Core analyses results along with the description on the lithology of the samples have been tabulated in Tables 1 and 2 for core samples from the Lone Rock and the Aberfeldy Pool respectively. These tables show the depth interval and the footage represented by every sample analyzed for porosity, liquid permeability, and oil and water saturation. Representative samples were taken at every visible change in the sand characteristic for the core obtained from the Aberfeldy Pool due to frequent inhomogeneity in the sand lithology from the depth interval of 1710 feet to 1725 feet. From the depth interval of 1725 feet to 1730 feet, it was generally a fine unconsolidated sand, and therefore, representative samples were collected at regular intervals of every half foot. For the core obtained from the Lone Rock pool, samples were taken at regular intervals of every one foot. These results are also plotted against the self-potential, and the resistivity logs on the corresponding wells in Figures 6 and 7. To simplify

ABERFELDY POOL

ELECTRIC LOG WITH CORE ANALYSIS RESULTS

POTENTIAL - MILLIVOLTS

160 120 80 40 0

RESISTIVITY - OHMS $M^2/M$

0 4 8 12 16 20

DEPTH IN FEET

1650
60
70
80
90
1700
10
20
30
40
1750
60
70
80

---- 16" LATERAL
—— 18" NORMAL

0 200 400 600 800 1000 1200 1400 1600

PERMEABILITY, K, mds.

10 20 30 40

POROSITY, Ø, PERCENT

80 60 40 20

OIL SATURATION, $S_o$, PERCENT

FIGURE 6

LONE ROCK POOL

ELECTRIC LOG WITH CORE ANALYSIS RESULTS

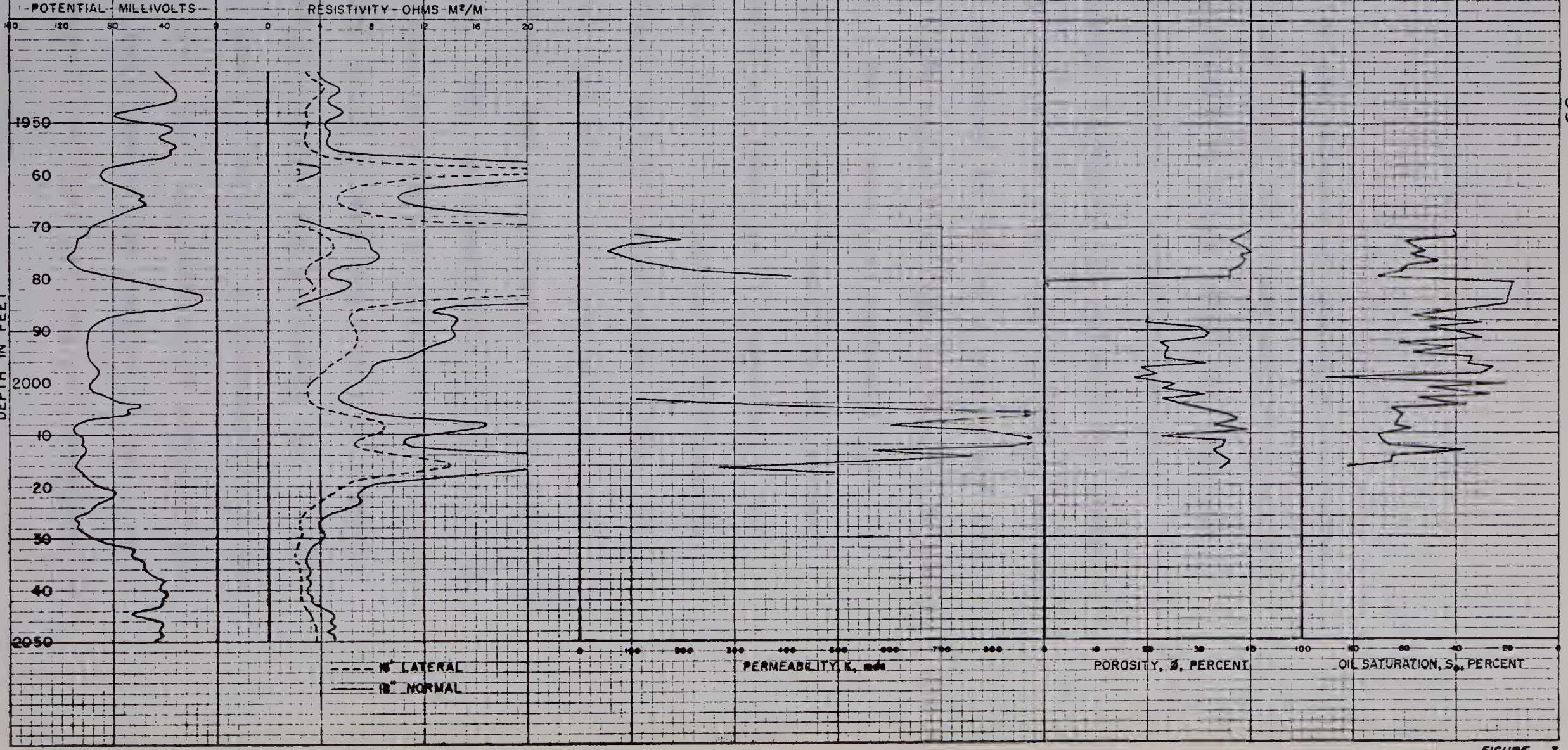


FIGURE 7

the comparison for the purpose of quantitative correlation with electric logs, the cores were divided into various zones according to their lithology with the help of log interpretation. Arithmetic weighted average permeability, porosity and saturation, along with the description on the lithology for these various zones have been tabulated in Tables 3 and 4, and illustrated against their respective logs on Figures 8 and 9.

Tables 1 and 2 show that measured porosity and permeability values vary from 20 to 40 percent, and from 50 to 3000 millidarcies, respectively, for different samples. Such a variation in the results is attributed mainly to the differences in the lithology of the cores, its shale and clay content, the amount of cementation and nonuniformity in the particle size distribution. For the consolidated portion of the core (representative feet 1985.0 to 1993.0 for the core from the Lone Rock Pool) it was noted that both porosity and permeability values are extremely low. The average porosity was 2.0 percent, and permeability less than 1.0 millidarcy. Such low values for porosity and permeability for this particular portion of the core are attributed mainly to tight packing and considerable

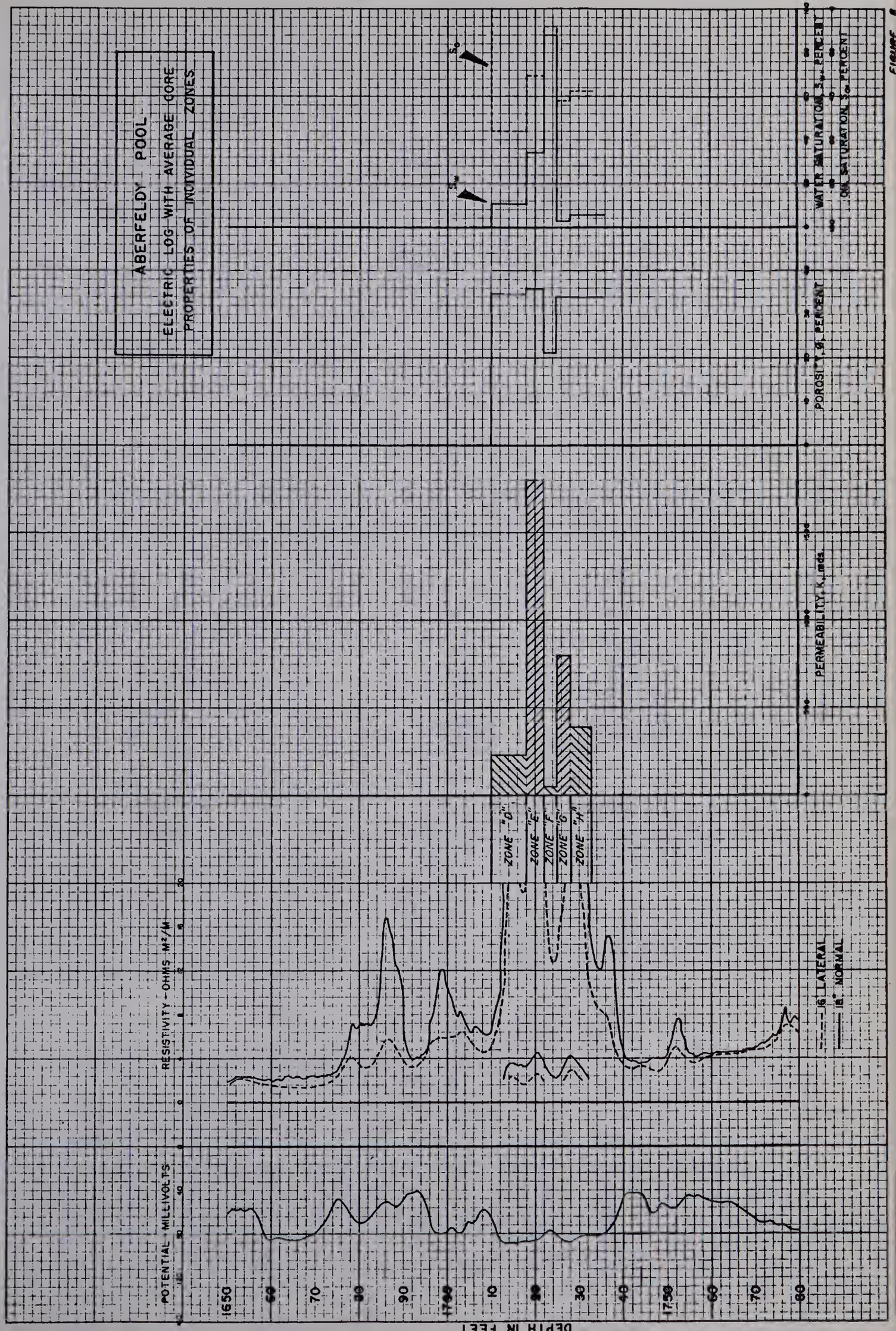
ABERFELDY POOL
ELECTRIC LOG WITH AVERAGE CORE PROPERTIES OF INDIVIDUAL ZONES
POTENTIAL - MILLIVOLTS
RESISTIVITY - OHMS M²/M
PERMEABILITY, K, mds.
POROSITY, ø, PERCENT
WATER SATURATION, Sw, PERCENT
OIL SATURATION, So, PERCENT
ZONE "D"
ZONE "E"
ZONE "F"
ZONE "G"
ZONE "H"
16" LATERAL
16" NORMAL
DEPTH IN FEET
1650
1700
1750

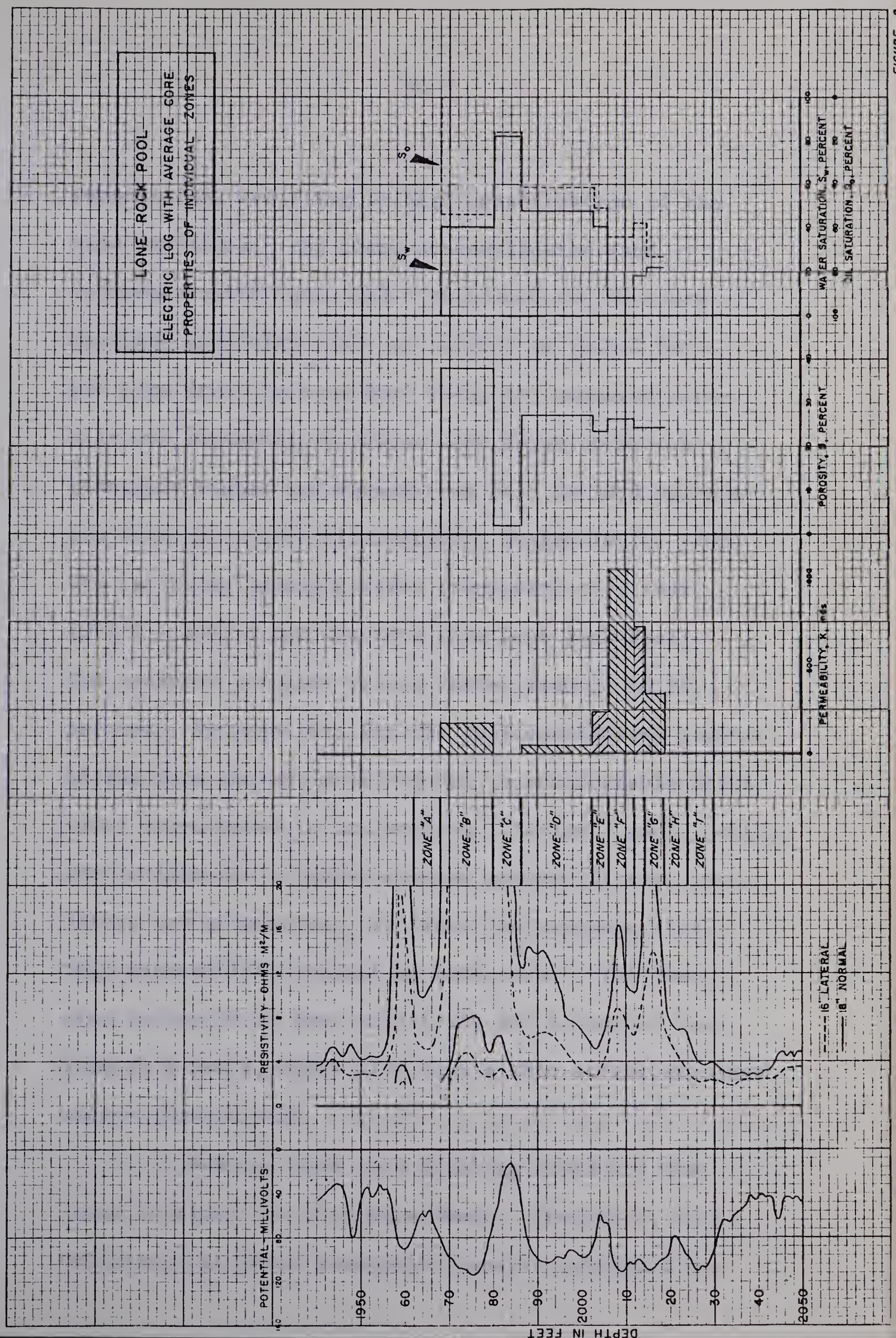
LONE ROCK POOL
ELECTRIC LOG WITH AVERAGE CORE PROPERTIES OF INDIVIDUAL ZONES
POTENTIAL - MILLIVOLTS
RESISTIVITY - OHMS M²/M
DEPTH IN FEET
1950
2000
2050
ZONE "A"
ZONE "B"
ZONE "C"
ZONE "D"
ZONE "E"
ZONE "F"
ZONE "G"
ZONE "H"
ZONE "I"
PERMEABILITY, K, mds
POROSITY, ϕ, PERCENT
WATER SATURATION, $S_w$, PERCENT
OIL SATURATION, $S_o$, PERCENT
$S_o$
$S_w$
16" LATERAL
18" NORMAL

FIGURE 9

cementation, resulting in high consolidation of the sand particles. For clean unconsolidated sand (representative feet 1719.0 to 1724.0 for the core from the Aberfeldy Pool, and 2010.0 to 2020.0 for the core from the Lone Rock Pool) the measured porosity and permeability values were found to be considerably higher and varied from 34.0 to 38.0 percent and from 50 to 3000 millidarcies, respectively. For the semiconsolidated portion (representative feet 1993.0 - 2007.0 for the core from Lone Rock Pool) the measured porosity values varied from 20 to 25 percent. Permeability for the semiconsolidated portion of the core was not measured due to considerable difficulty encountered in the packing. Tables 3 and 4, which show arithmetic weighted average permeabilities, porosities and saturations, indicate the presence of a high permeability channel in both cores. This was also indicated on the resistivity and potential log. Figures 8 and 9, which also show a thin streak of clean unconsolidated sand.

Mud was used as a drilling fluid for the cores obtained for this experiment. Therefore, it is believed that water saturation results tabulated in

Table 2, are relatively high. Values as high as 80 percent were assumed to be due to the invasion of mud filtrate at the time of drilling. The oil saturation figures obtained, are in fact, probably low because of flushing of the initial oil by the invaded fluid, and complete loss of solution gas, due to the reduction of pressure. The measurement of fluid saturation by numerous core analyses techniques has proven to be inaccurate for two major reasons. The principle difficulties in obtaining core samples (13), of which the fluid content represents conditions existent within a reservoir are: 1) Contamination and flushing of the cores by the drilling fluid, or liquid phase, therefrom; 2) reduction of pressure occuring as the cores are withdrawn from the well, and resulting in expulsion and loss of portion of native fluids. High water saturation is obtained by core analysis when water base mud is employed as a drilling fluid and reverse is true when oil is utilized for the purpose as a drilling fluid.

The water saturation values tabulated in Table 1, are appreciably low. The reason for such a low water saturation might be explained by the fact that these particular cores were removed from the rubber sleeves

beforehand, and stored in glass bottles. It was observed later on, that these bottles were not air tight, and part of the water had evaporated. To validate this, a few samples from the core from the Lone Rock Pool were analyzed after they had been stored in glass bottles for a few days. The results were appreciably lower than the initial water saturations obtained for these samples. Thus, it was found essential to analyze the core samples for their fluid content as soon as they were removed from the rubber sleeve.

The importance of obtaining the fluid content approximately representing the conditions existent within a reservoir from the quantitative interpretation of electric logs, has been realized in the petroleum industry for the past number of years. In the routine coring of oil formations, it is impracticable either to exclude the possibility of contaminating cores with water, or oil, or to determine the extent of such contamination. It was therefore, desireable to know the existing amount of water saturation in a formation from the quantitative interpretation of logs.

Numerous correlation (10, 11) of the type shown in equation (5) have been published in the literature for

determining water saturation from the electric logs for the consolidated sands. Insignificant amounts of work have been done in this direction for the unconsolidated sands. Such an attempt here was proven to be unsuccessful due to an insufficient number of samples, and lack of formation resistivity factor data. The few formation resistivity factors (14), which were available from the previous experiments on this sand were insufficient. The necessity to measure formation resistivity factors experimentally in the laboratory for each individual sample was recognized. It was found that with the measured porosity on the corresponding samples, a reasonably accurate value for "m" could be calculated from the Archie's formula, equation (2). Further work in this direction would certainly provide useful information for correlation purposes of unconsolidated sands. It has been proven that reasonably accurate values for porosity could be easily measured in the laboratory, or could be accurately assumed or obtained from the porosity logs, for an unconsolidated formation. From the known value of "m", "F" could be calculated for that particular formation, and utilized in equation (6) to determine SW.

Looking at the permeability results for every core sample, it was observed that the values varied appreciably from sample to sample. Initially it was thought that such variation was a result of differences in the degree of packing. To study this, more than two or three samples were prepared for the permeability measurements from the same one foot core sample, with plugs obtained at the distances of only half an inch apart. This was done for ten core samples at different intervals.

| Sample No. | Plug No. 1 | Plug No. 2 | Plug No. 3 |
|---|---|---|---|
| 2 | 106 | 101 | 104 |
| 3 | 195 | 200 | 193 |
| 5 | 51 | 53 | 49 |
| 9 | 227 | 231 | 221 |
| 10 | 409 | 415 | 401 |
| 43 | 840 | 832 | 850 |

Perusal of the above table indicates that the results could be duplicated within reasonable accuracy with an error less than five percent. To further explain such a variation in the results, the shale content of the few samples were varied. A considerable difference in the permeability was noted. By removing a few shale

particles from the sand, a noticeable increase in the permeability was obtained. On the other hand, by adding few extra shale particles the permeability of the sample was decreased drastically. For example, the permeability of sample No. 3 (Lone Rock core) was measured to be 195 millidarcies, but by removing a few shale and clay particles, the permeability increased to 610 millidarcies, an increase of more than three fold.

The prediction of permeability from the quantitative interpretation of various logs proved uncuccessful. Various experiments have been performed in the past several years, and a number of correlations have been derived. So far no reliable correlations have been obtained, either for the consolidated or the unconsolidated sands. More attention is being focused on the laboratory measurements of the permeability on core samples. In the case of a consolidated formation, the task is simple and straightforward, but becomes complicated for the unconsolidated sands. The question of primary importance in the case of an unconsolidated formation arises as how well a core sample could be simulated to represent original reservoir conditions.

From the study of permeability (15, 16, 17, 18, 19) on the natural sand, glass beads, and Ottawa sands, it has been concluded that the permeability of an unconsolidated sample is effected by the following:

1) Size and shape of the particles.
2) Variation in the shape and size of the particles.
3) Type of packing and arrangement of the particles.
4) Different degree of packing.

The sand employed in this experiment was in its natural form, and as the primary object here was to determine the permeability of this sand in its native state, effects of size and shape, and variation in size and shape of the particles were not considered. As for the arrangement of the particles, sufficient care was taken not to disturb the original arrangement of the shale and sand particles present in the core sample. To study the effect of the arrangement of the particles, a few samples were repacked in a random manner.

| Sample No. | Undisturbed Packing | Random Packing |
|---|---|---|
| 10 | 409 | 442 |
| 43 | 840 | 798 |

From the perusal of the previous table it is noted that a maximum of only ten percent difference in the permeability was realized. The only question of any doubt is therefore, the degree of packing, as to whether it really represented the actual overburden pressure of the reservoir. To simulate these conditions, the samples were packed under a pressure equivalent to overburden pressure, and therefore, it is believed that reasonably representative packing was obtained by this method. Thus, it was concluded that the presence of the shale, and silt particles, and their amount, had greater effects on the permeability of the sand.

Another possible source of error in the permeability determination was the type of fluid used. Bubbles of gas in the sample when water was used is one such source of error. This was prevented by deaerating the water by evacuation. Another source of error was silt and clay particles in the water. This was remedied by using distilled water. A rather serious source of error in the permeability determination with liquid was the swelling of clay minerals in fresh water. This has been proven to be very pronounced in some cases, especially when the sand contains numerous shale and clay particles.

This was taken care of by dissolving chemically pure sodium chloride in the distilled water to simulate the salinity of the formation water.

Permeability values for a number of samples are missing in Tables 1 and 2. In a few cases no representative sample could be obtained due to the presence of numerous thin shale and sand breaks. No measurements were taken when the sand was consolidated or in the form of siltstone. In case of a semiconsolidated sample, it was difficult to obtain a large enough representative sample to hold in the coreholder. Attempts were also made to determine vertical permeability of the core without disturbing the sand from its original state. Due to the presence of numerous small and large shale breaks, it was difficult to maintain any vertical flow even at a very high pressure. The result was that there was no vertical permeability in almost all of the samples examined.

Porosity values for the unconsolidated sand shown in Tables 3 and 4, varied from 34 to 39 percent. This range of measured porosity agrees favourably with other experimental results on natural sand, glass beads, and Ottawa sands. It has been shown that for a single

component system composed of spherical particles of approximately same size, the porosity does not vary with size, but is dependent only on different types of packing. For a multicomponent system consisting of spherical grain of various sizes, the porosity is dependent on the size distribution, particles size, and type of packing. It is also shown that there are three geometrically simple ways of stacking either square layers or simple rhombic layers upon one another. There are, therefore, three geometrical schemes of systematic packing for each of the two simple types of layers, making six types in all. Two of these types are orientation varients, but four are independent arrangements. For the cubicle or the loosest type of packing, the porosity has a value of 47.64 percent. For the tightest or rhombohedral packing, the porosity is 25.95 percent. The other types of packing have values of porosity intermediate between these extremes. According to Muskat (20) sand particles with grain size distribution, similar to that used in this experiment, should have a porosities of approximately 40 percent. Francher, Lewis, and Barnes (21) give a value of 34.5 percent for a multicomponent system of average size distribution. It, therefore, was concluded, by the

present author, that the range of values for porosity obtained in this experiment, represents true average values for an assemblage of unconsolidated sand particles in their native state.

Sieve analyses were carried out on every sample to determine grain size distribution. A tyler sieve analysis is shown in Table 5 for four samples with different size distributions. The mesh size in inches has been tabulated against the percent weight of each size retained on the screen. A plot of cumulative mass fraction through versus aperture diameter for these samples has been shown in Figures 10 to 13. These curves indicate that the distributions vary from uniform ( Figure 10) to one of completely nonuniform nature (Figure 11, 12, and 13). Figure 10, which shows uniform size distribution for sample no. 6, indicates that major portions of the particles, more than 80 percent, are coarser than 140 mesh. Figures 11 and 12, which show nonuniform size distribution for sample no's. 3 and 12, indicate that more than 60 percent of the particles are finer than 200 mesh. This nonuniformity in size distribution, along with various amounts of clay and shale present in core samples mainly accounts for the wide variation in the porosity and the permeability results.

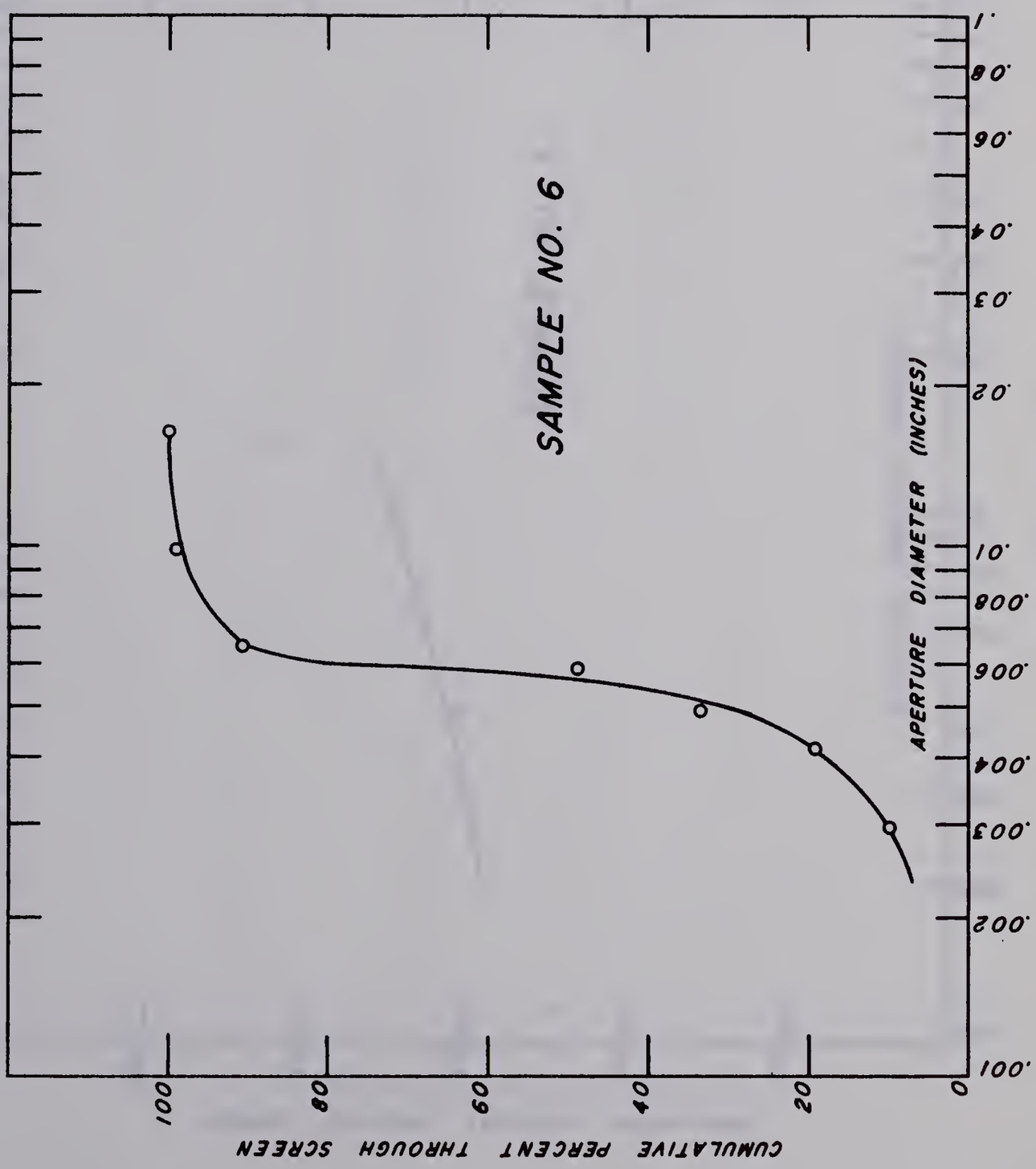


FIGURE NO. 10

APERTURE DIAMETER VERSUS PERCENT THROUGH

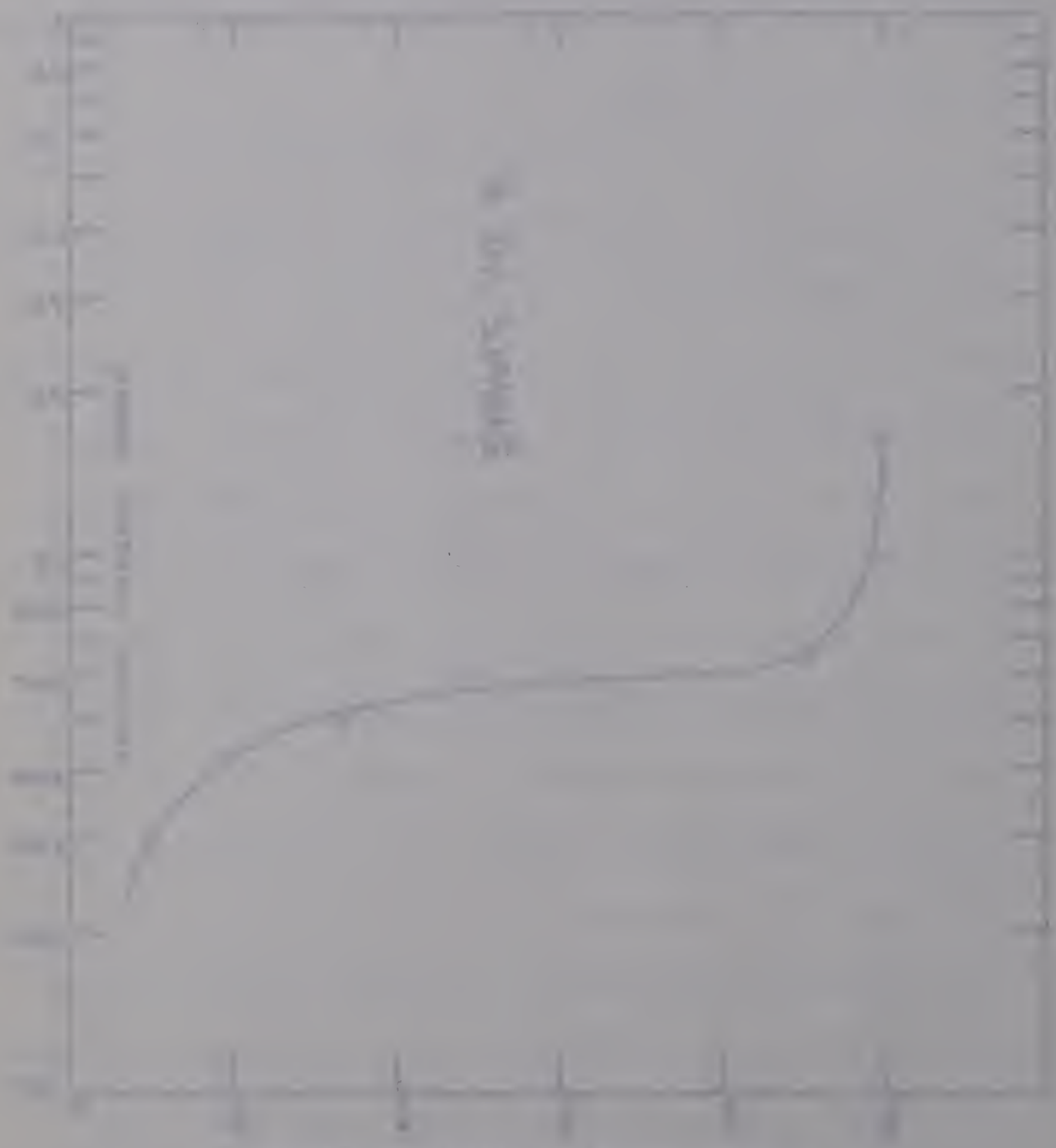

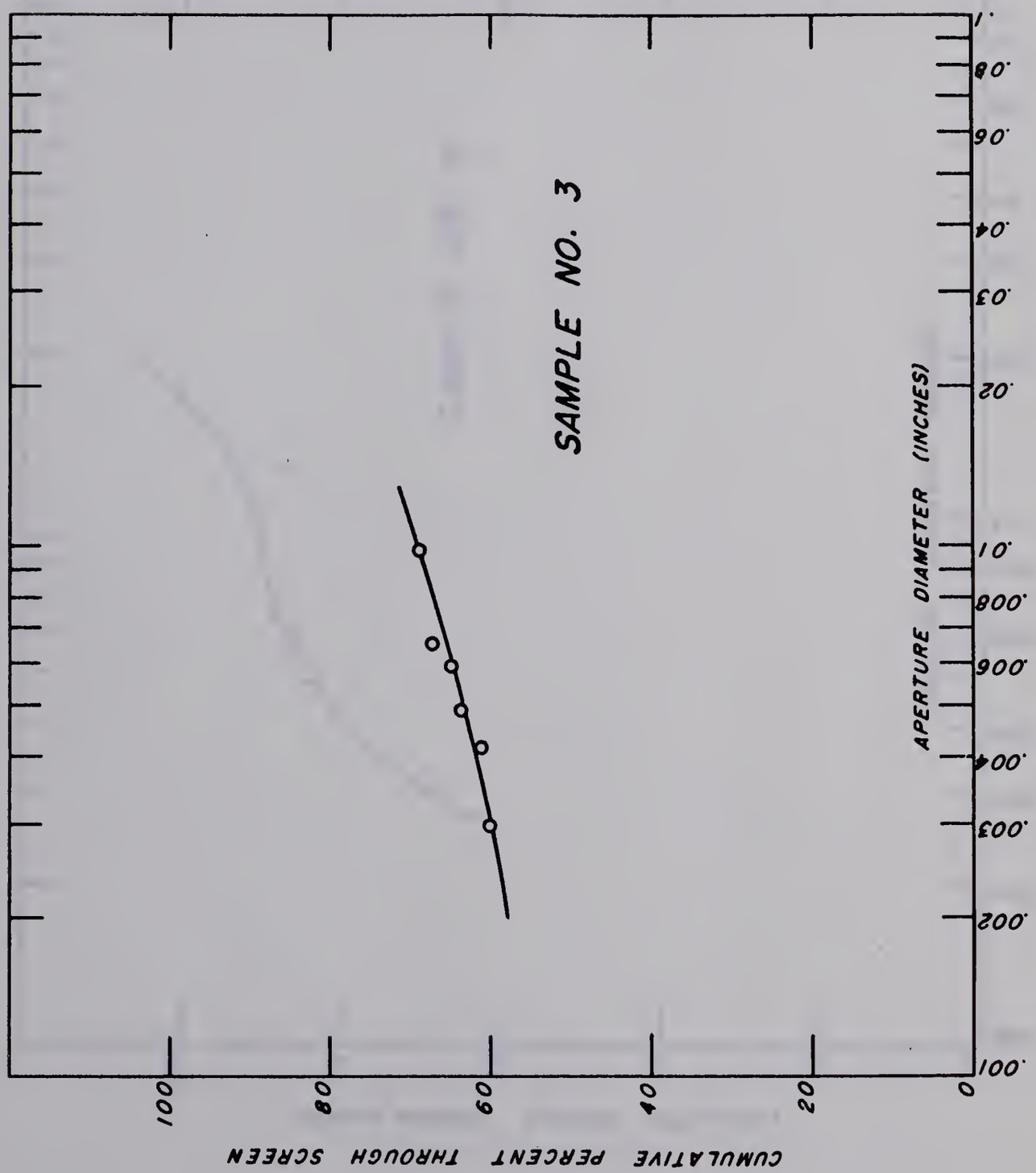


FIGURE NO. 11

APERTURE DIAMETER VERSUS PERCENT THROUGH

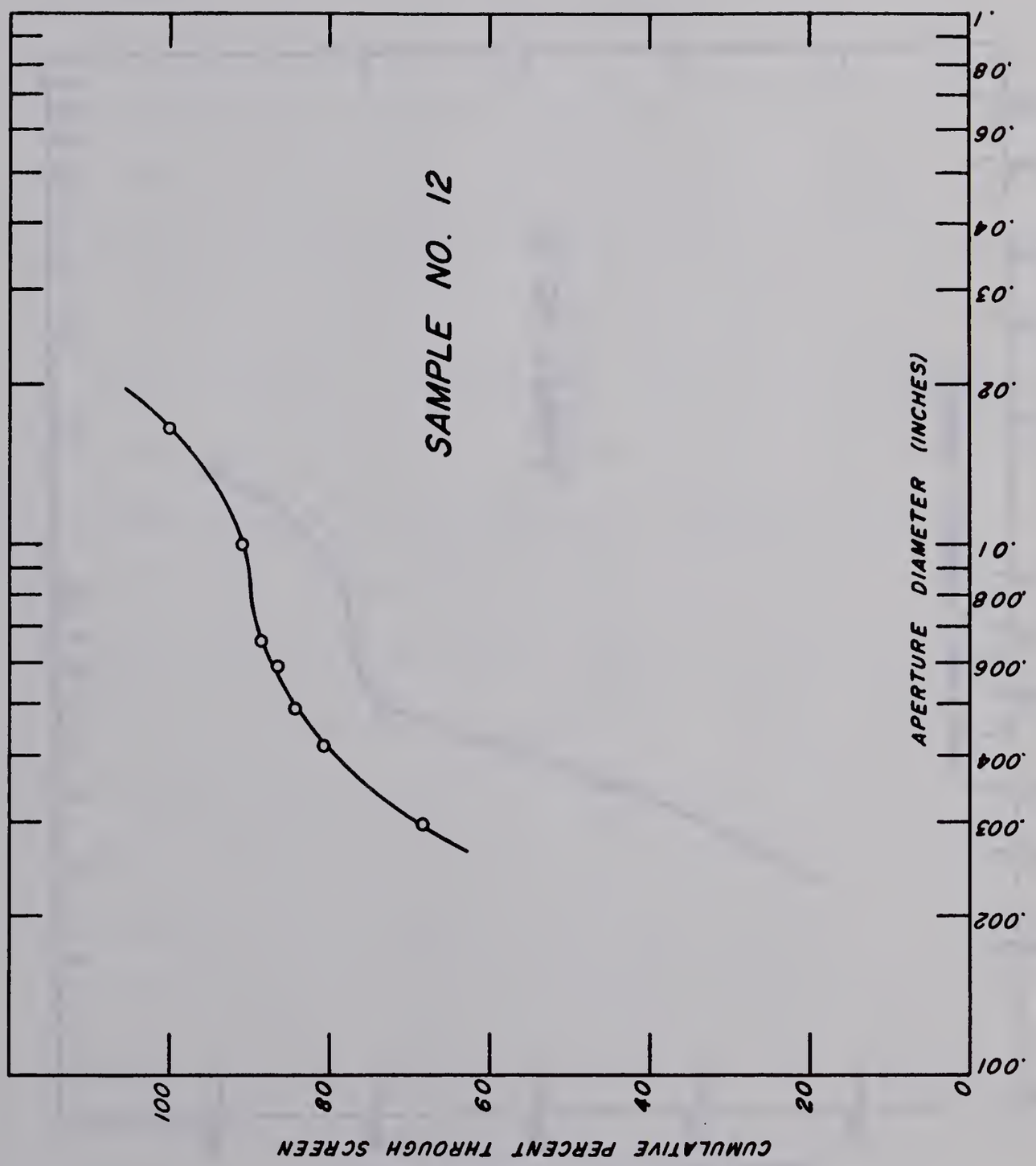


FIGURE NO. 12

APERTURE DIAMETER VERSUS PERCENT THROUGH

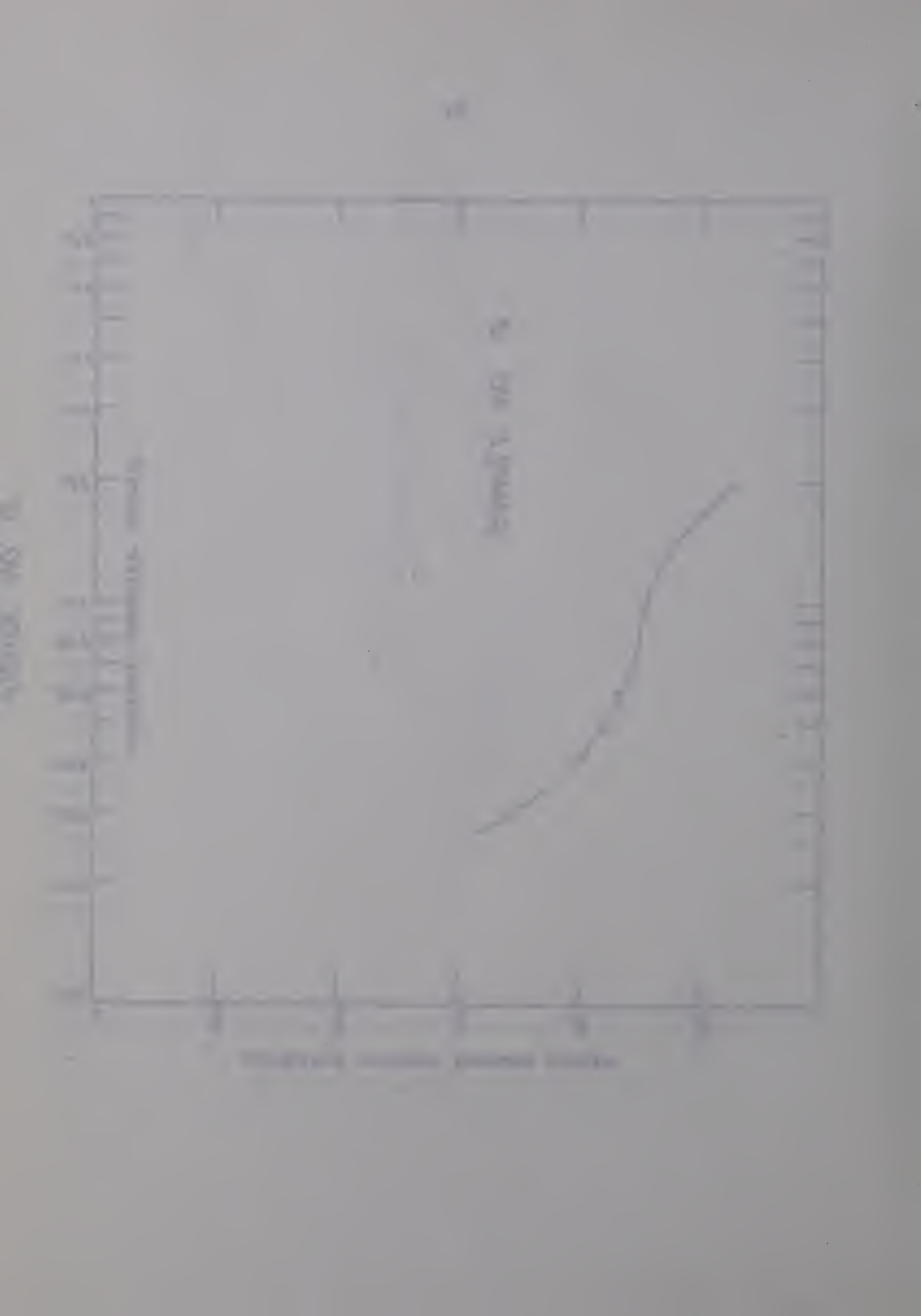

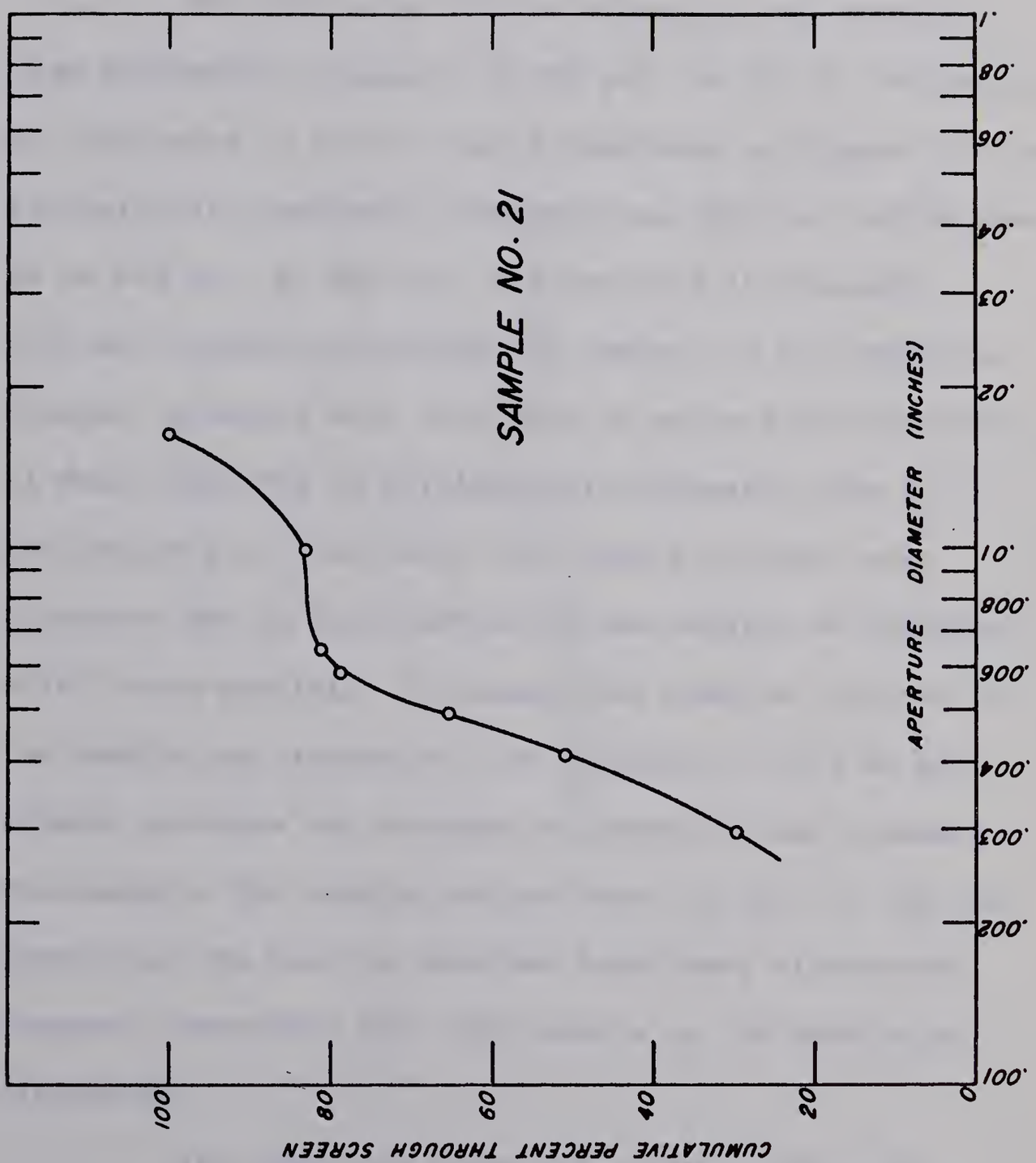


FIGURE NO. 13

APERTURE DIAMETER VERSUS PERCENT THROUGH

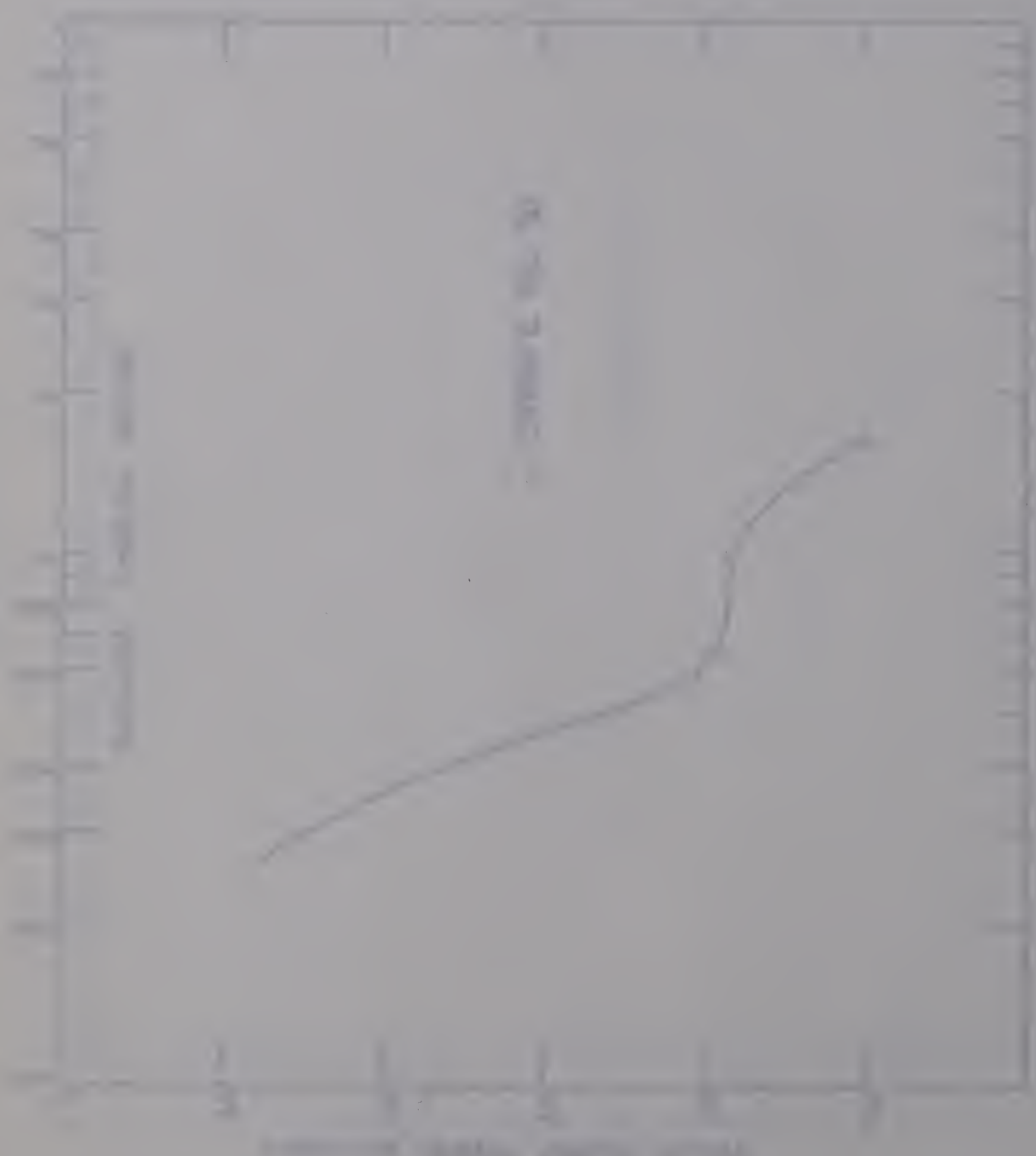

VISCOSITY

The viscosity of dead crude oil was measured from atmospheric pressure to 900 psi. at 75° F. The results are tabulated in Table 6 and illustrated in Figure 14. The viscosity at atmospheric pressure was 750 cps. and increased to 869 cps. at 900 psi. The increase in viscosity with an increase in pressure is typical of all newtonian liquids. Attempts were also made to measure the viscosity of dead crude oil on Rolling-ball viscometer. Due to the presence of free water the results obtained were erroneous and no duplications of the results on different trials were possible. To compare the results obtained on the Bendix-lab viscometer, the viscosity of oil at atmospheric pressure was measured on several other standard viscometers. The results varied from 745 cps. to 755 cps. Therefore, the results obtained from these viscometers compared favourably with the results on the Bendix-lab viscometer.

The term dead crude oil, meaning crude oil with no gas in solution, used in the discussion here is misleading in that the crude oils have tendency to loose their light hydrocarbons for a considerably long period of time when exposed to atmosphere. It was noted in this

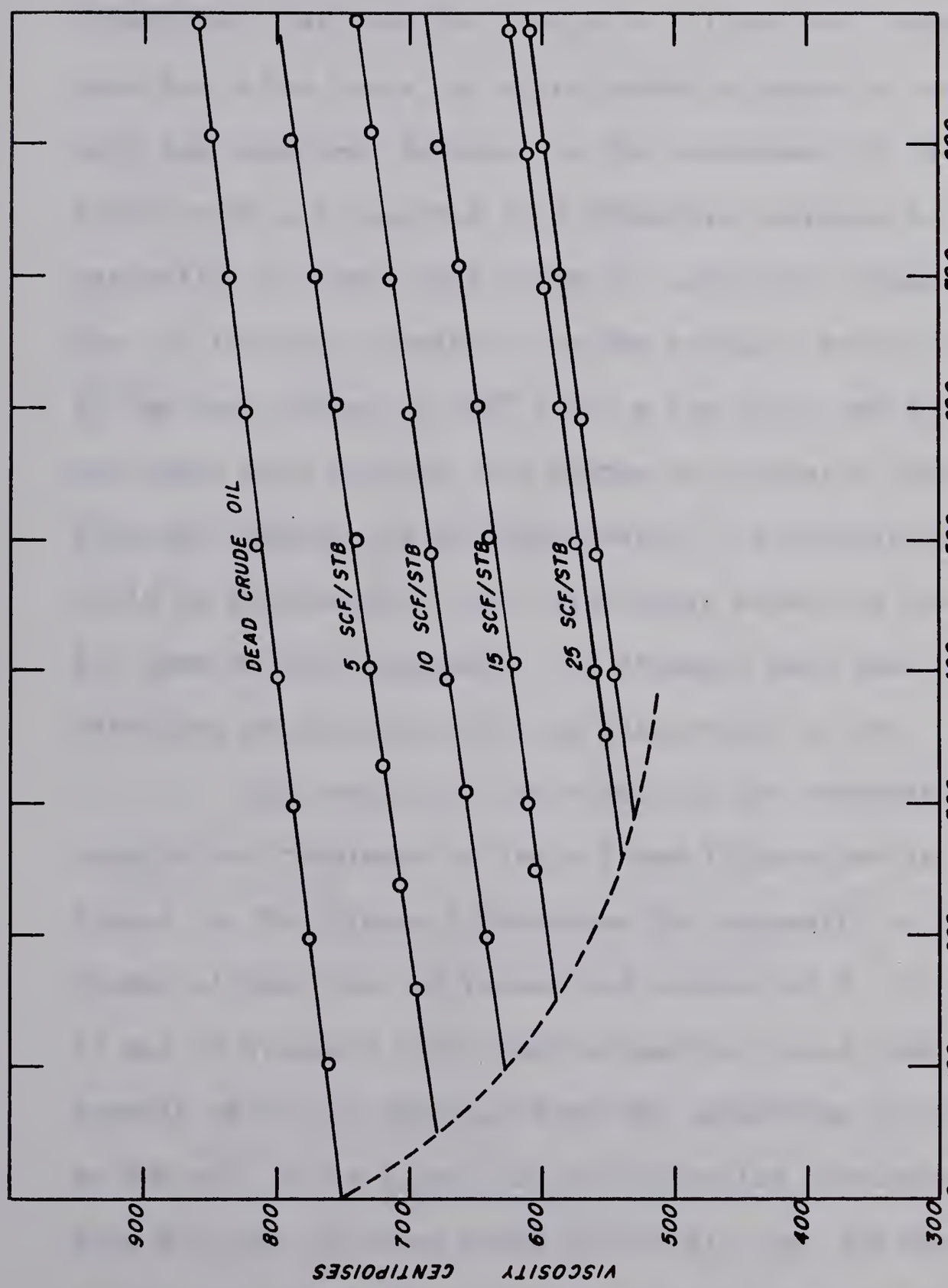


FIGURE NO. 14

VISCOSITY OF DEAD CRUDE OIL AND RECOMBINED SAMPLES AT DIFFERENT PRESSURES

experiment that when the sample of oil was left exposed even for a few hours, an appreciable increase in viscosity was observed. Exposure to the atmosphere of this heavy crude oil resulted in a threefold increase in viscosity. The term dead crude oil used here stands for the oil that was obtained from the refinery treater, where it had been heated to 200° F for a few hours and gas and water were removed. The change in viscosity with time and exposure to the atmosphere, to a certain degree, could be attributed to the thixotropic nature of the crude oil used in this experiment. No attempts were made to determine whether this oil was thixotropic or not.

The results of the viscosity for recombined samples are tabulated in Table 6 and illustrated in Figure 14. The figure illustrates the viscosity of dead crude oil with that of recombined samples of 5, 10, 15, 25 and 30 standard cubic feet of gas per stock tank barrels of oil in solution from the saturation pressure to 900 psi. It is noted that the viscosity decreases from 825 cps. for dead crude oil to 610 cps. for the sample with 30 standard cubic feet of gas per stock tank barrel of oil. A cross plot of figure 14 is shown in Figure 15 at 600 psi. This figure illustrates the decrea-

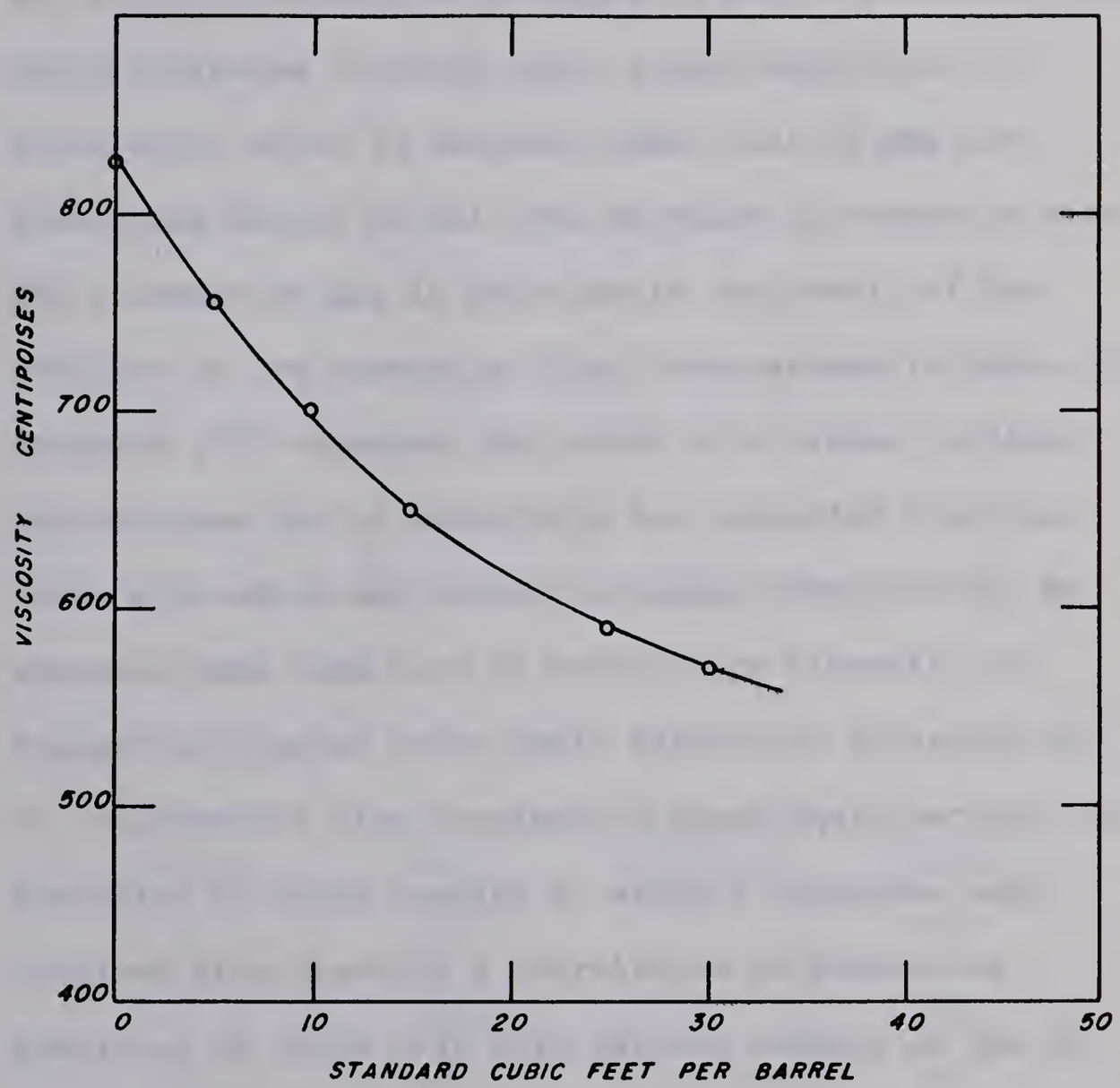


FIGURE NO. 15

VISCOSITY OF OIL WITH DIFFERENT AMOUNTS OF GAS IN SOLUTION AT 600 POUNDS PER SQUARE INCH PRESSURE

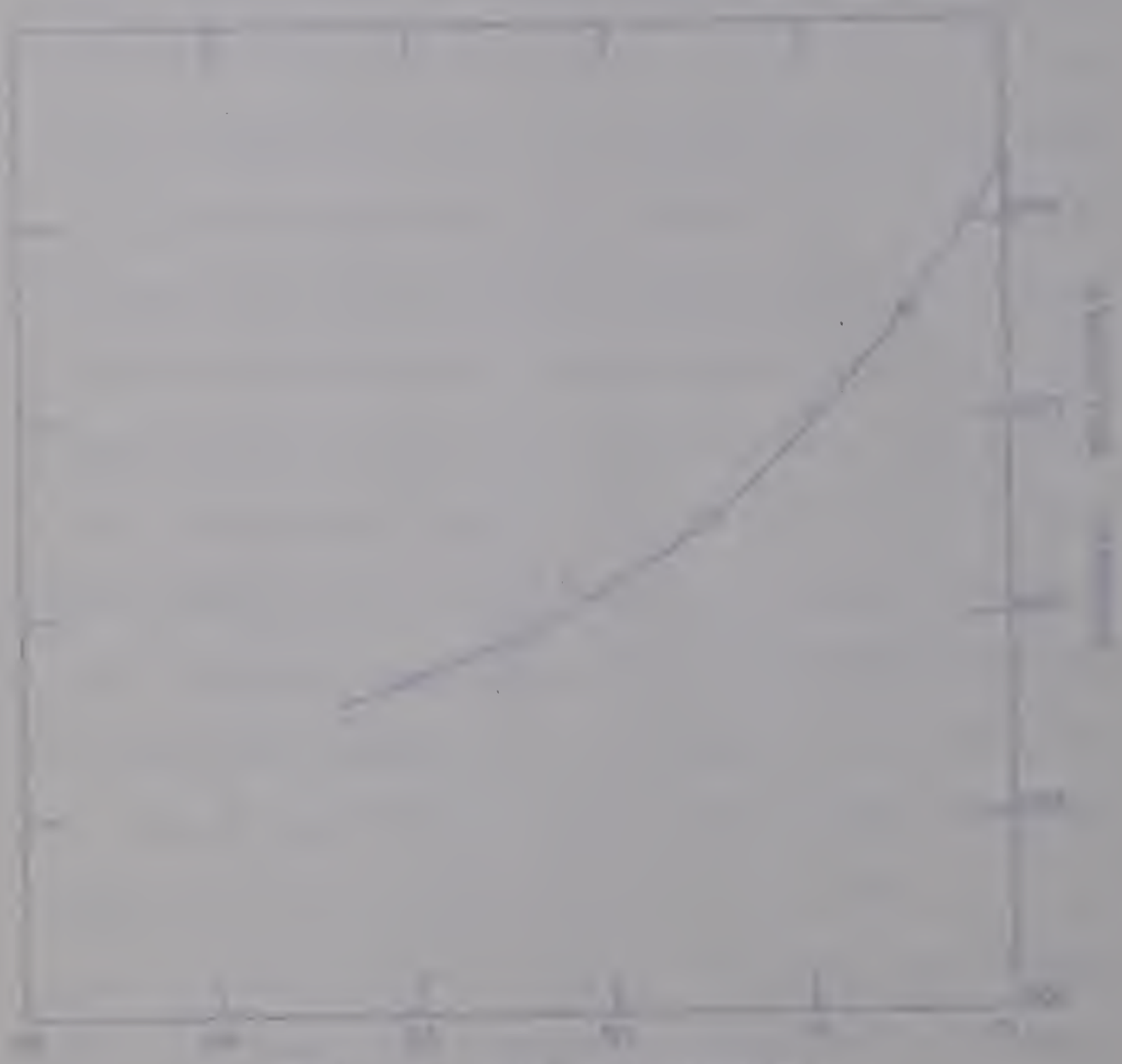

se in viscosity with an increase in gas in solution. The curve indicates a fairly steep slope which tends to flatten out after 25 standard cubic feet of gas per stock tank barrel of oil. The decrease in viscosity with the increase in gas in solution is the result of the addition of low viscosity light hydrocarbons in crude oil. Standing (22) observed that crude oils richer in light hydrocarbons are of relatively low viscosity than the crude oils which are richer in higher hydrocarbons. No attempts were made here to measure the viscosity of recombined samples below their saturation pressures due to considerable time required to reach equiliberium. The densities of these samples at various pressures were obtained from Standing's correlation of predicting densities of crude oils with various amounts of gas in solution.

A number of workers have attempted to establish a correlation for viscosity with the gravity of the crude oil and the amounts of gas in solution. Because of the varying composition of different crude oil, predictions of crude oil viscosity from simple correlations connot be made with extreme accuracy. Oil gravity and temperature are the most critical variables that effect crude oil

viscosity, the higher the temperature and gravity the lower the crude oil viscosity. The oil used in this experiment was of 12.5 degrees API gravity and Beal's (23) correlation gives a viscosity of 3000 cps. for 12.5 degrees API crude oil. The results obtained here were compared with other correlations but no duplications were possible for viscosity of dead crude oil. The values of viscosity obtained for 12.5 degree API crude oil from correlations were either too low or too high, as shown in the table below.

| API GRAVITY | VISCOSITY (CPS.) | | |
|---|---|---|---|
| | BEAL | JOHNSTON | TROSTEL |
| 10 | 1050 | - | 300 |
| 12 | 650 | 6000 | 200 |
| 14 | 400 | 1050 | 150 |
| 16 | 200 | 400 | 70 |
| 18 | 100 | 150 | 50 |
| 20 | 65 | 75 | 40 |

It has been shown that crude oils with negligible amounts of light hydrocarbons but with the same density have different viscosities depending on their compositions. Johnston and Sherborne (24) gave a relation

ship between crude oil viscosity at 100° F and oil gravity. The correlation includes, in part, results from Trostel's work, which presented an approximate relationship between API gravity and viscosity of more then 200 samples of California crude oils at 100° F. A plot has been made of 655 gas free samples of crude oil viscosity measurement at 100° F. The samples represent the viscosity of crude oil taken from 492 oil fields, of which 358 are in the United States. Trostel's (25) and Johnston's (26) temperature oil gravity relationship for California crude oils is shown on a graph by Beal (23) along with 655 plotted values. From these correlations it was obvious that the predictions of viscosity of heavy crude oil from its gravity resulted in considerable error.

In Figure 14 viscosity for the recombined samples were extrapolated to their respective saturation pressures. Points representing the viscosity of recombined samples at their corresponding saturation pressures are joined by a dashed line. This line approximately predicts the increase in viscosity as the solution gas comes out of solution below the bubble point pressure. The portion of the curve above the saturation pressure represents the increase in viscosity with increase in pressure on a

homogeneous saturated oil with its dissolved gas. Below the saturation pressure, the escape of gas from solution with a reduction in pressure increases the viscosity of the residual oil to a greater extent then it is reduced by the pressure decline, resulting in a net increase in viscosity. The saturation pressure of the oil is thus identified in the viscometer through the minimum in the viscosity pressure curve. The increasing slope of the viscosity pressure curve as the pressure approaches atmospheric reflects in part the increased richness of the liberated gas and loss of the more volatile fractions of oil. The solpe of the viscosity pressure curves vary from field to field with the nature of the oil and its dissolved gas.

## BUBBLE POINT PRESSURE

Figure 16 illustrates the pressure-volume relation at constant temperature for three recombined samples of 10, 15 and 30 standard cubic feet of gas per stock tank barrel of oil in solution. These results are also tabulated in Table 7. Data on other recombined samples were not obtained due to considerable length of time required to reach equiliberium. Based on visual observations of the first appearance of gas phase through

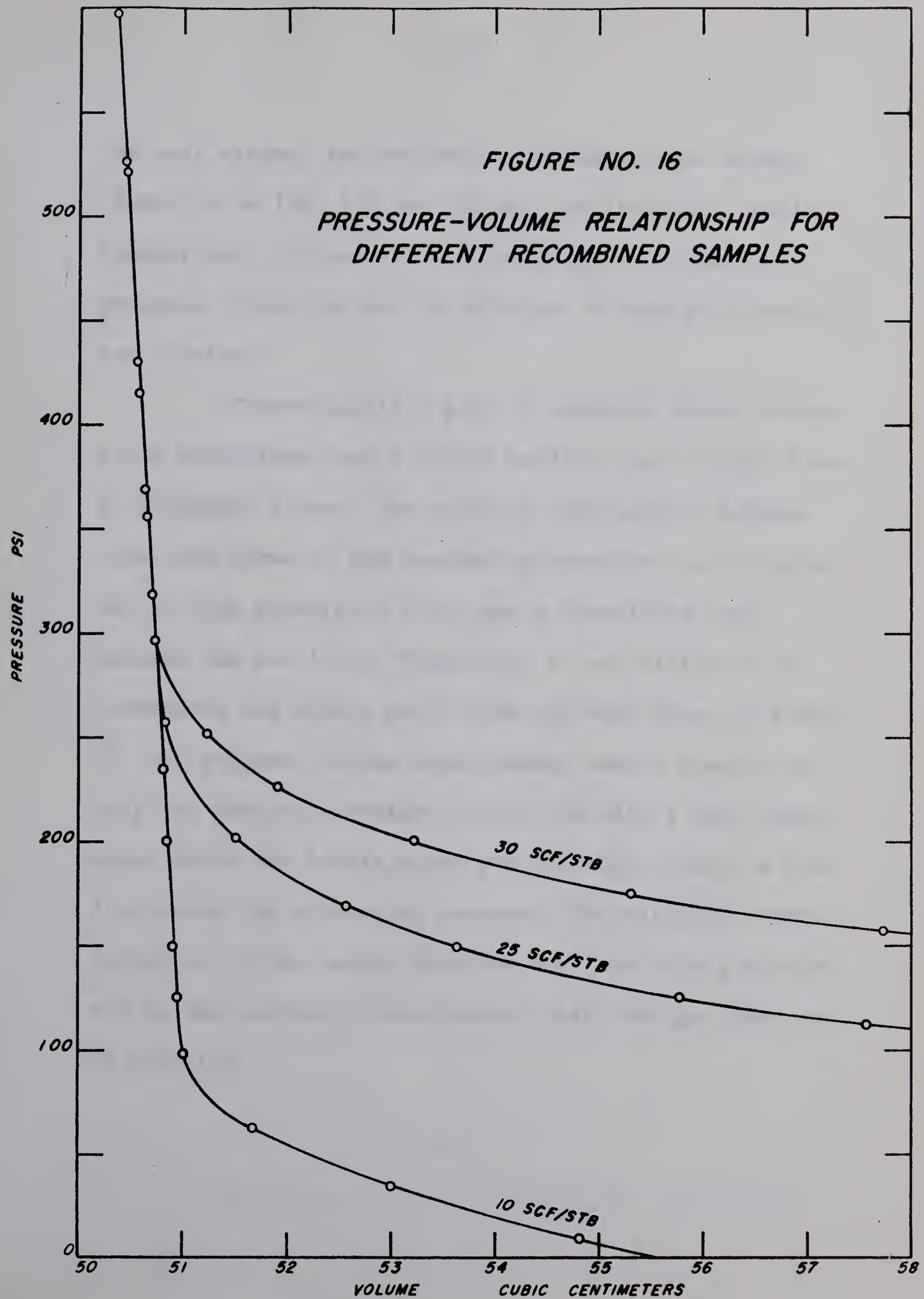
FIGURE NO. 16
PRESSURE-VOLUME RELATIONSHIP FOR DIFFERENT RECOMBINED SAMPLES
PRESSURE PSI
500
400
300
200
100
0
30 SCF/STB
25 SCF/STB
10 SCF/STB
50
51
52
53
54
55
56
57
58
VOLUME CUBIC CENTIMETERS

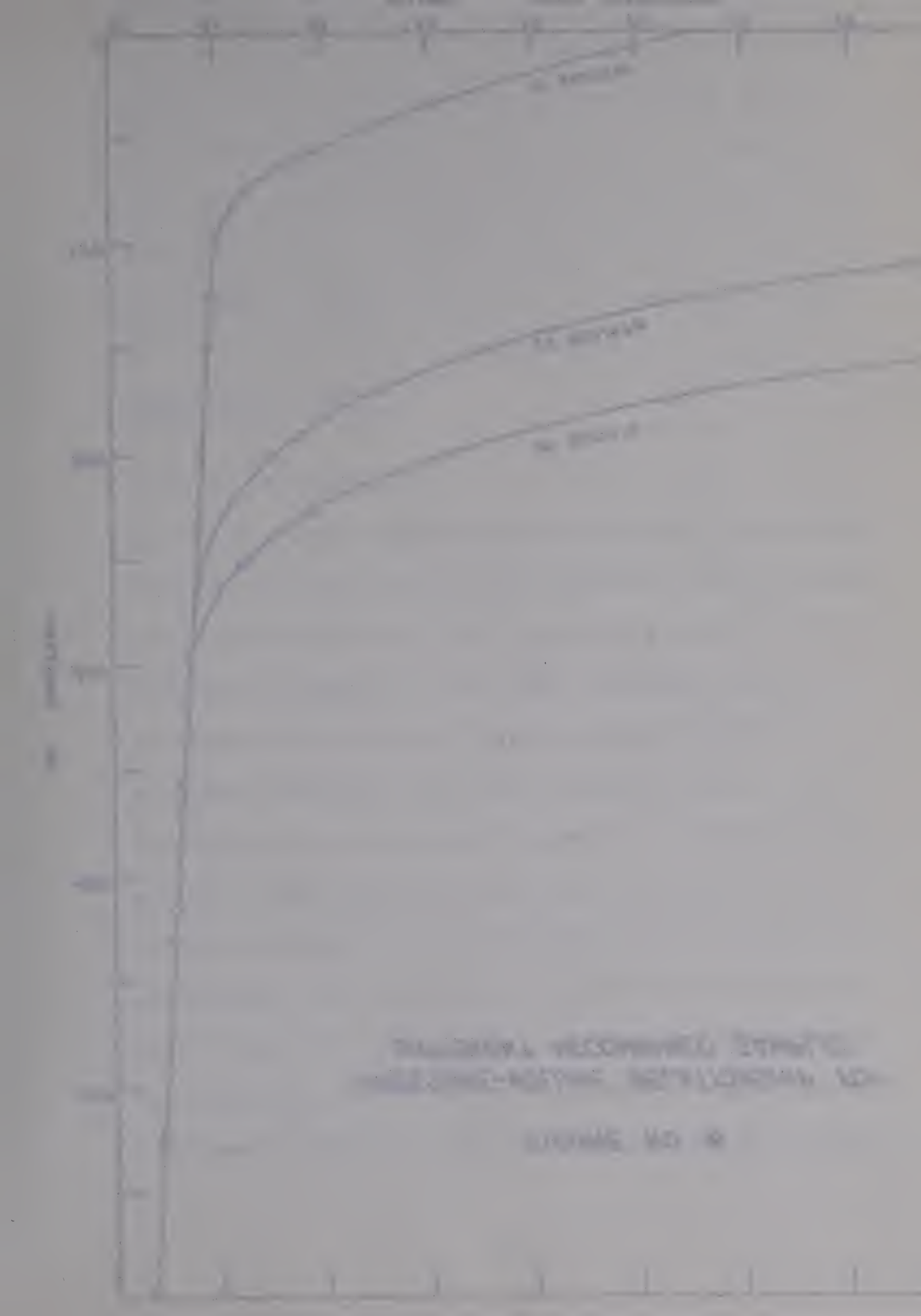

the cell window, the saturation pressures were established to be 100, 150 and 300 psi for the above samples, respectively. Figure 17 is a cross plot of saturation pressure versus the gas in solution. A straight line plot was obtained.

Theorotically a plot of pressure versus volume for a recombined sample should exhibit two straight lines of different slopes. The point of intersection between these two lines is the saturation pressure. As it turned out in this experiment there was a transition zone between the two lines. Therefore, it was difficult to interprete the bubble point from the data shown in Figure 12. The pressure volume relationship should consist of only two distinct straight lines, one with a very steep slope above the bubble point and the other almost a flat line below the saturation pressure. The different characteristics of the curves obtained here was mainly attributed to the extremely slow rate at which the gas came out of solution.

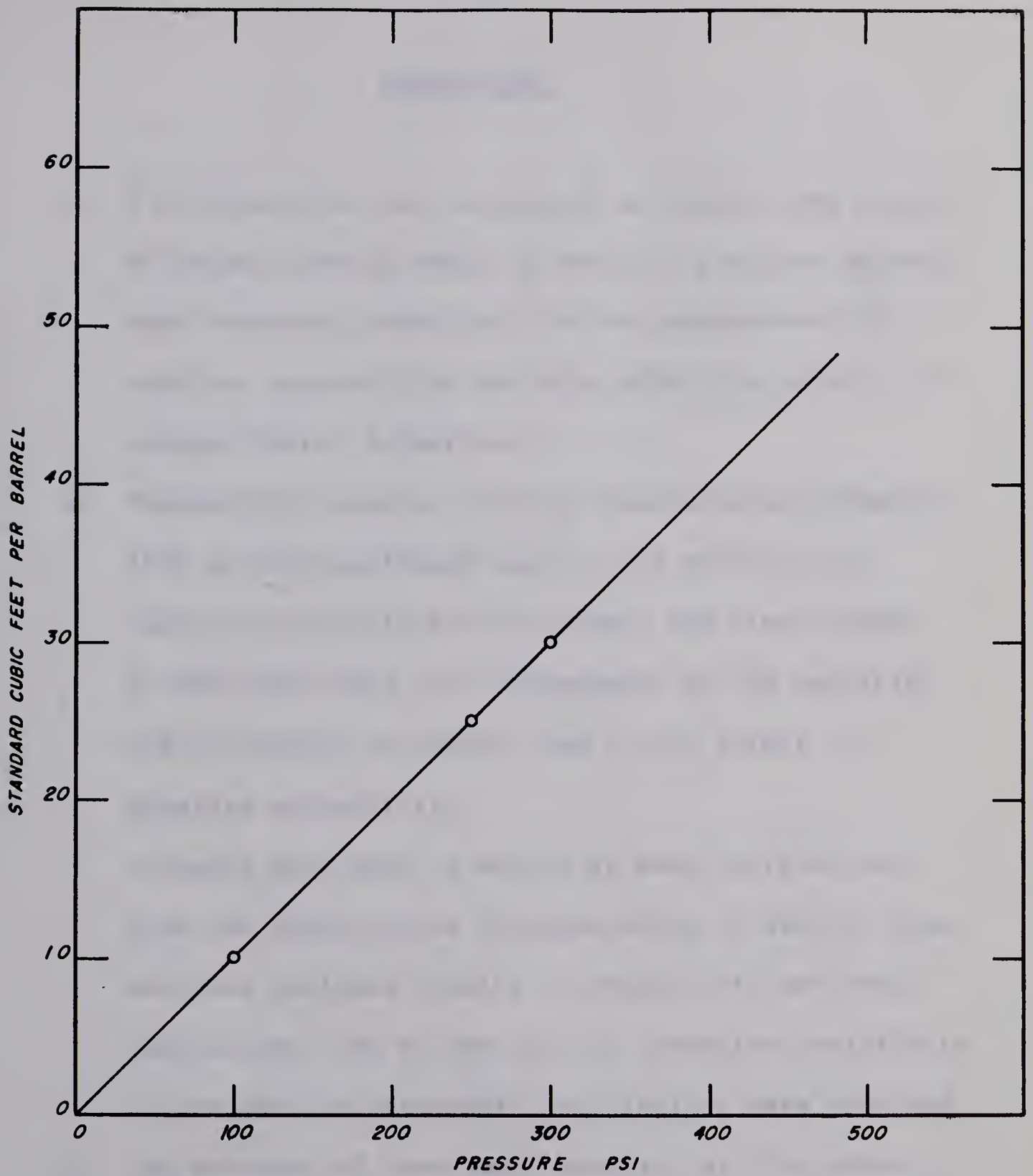


FIGURE NO. 17

GAS SOLUBILITY AT DIFFERENT PRESSURES

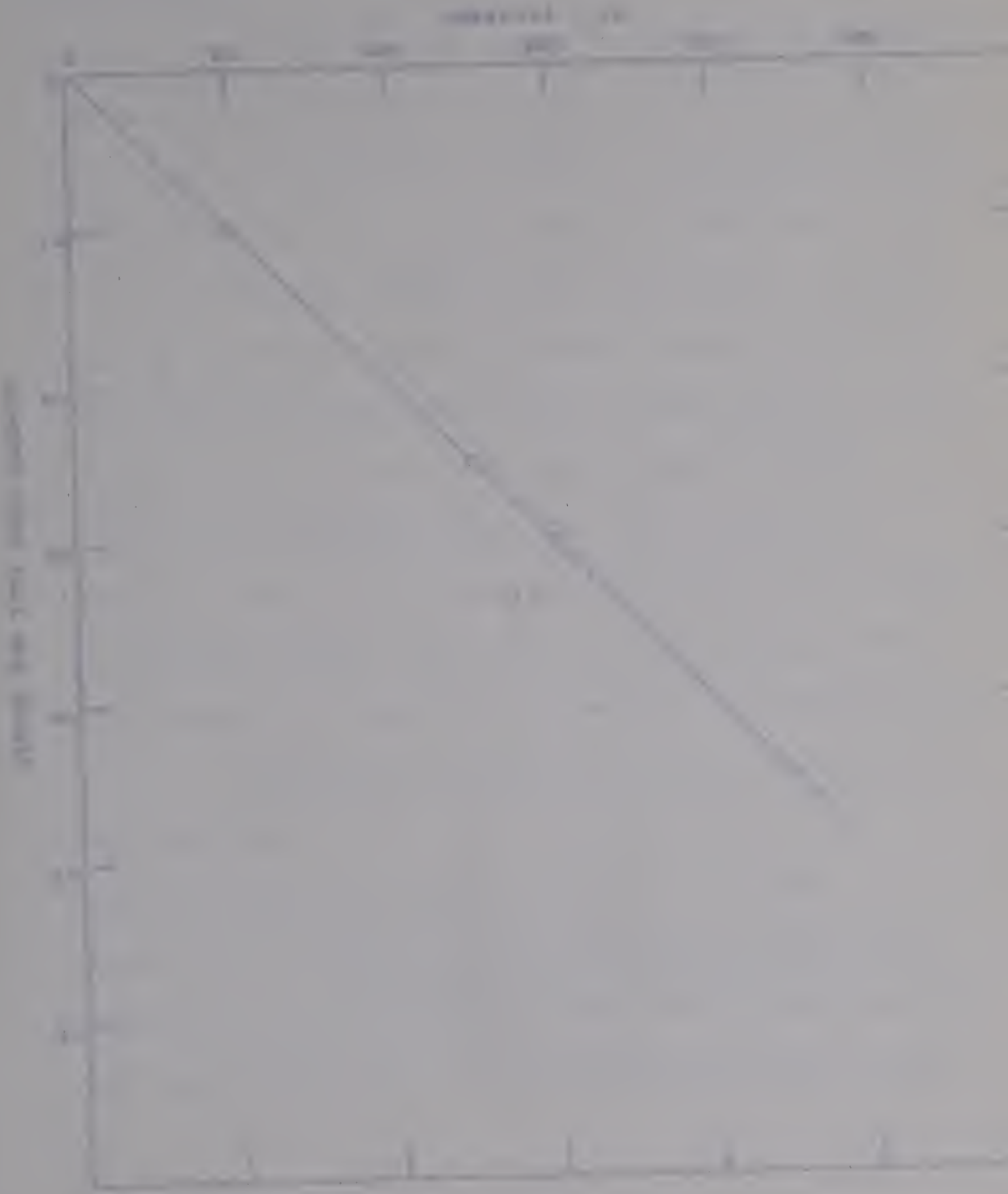

# CONCLUSIONS

1. A procedure has been developed to repack core samples of unconsolidated sands in order to simulate approximate reservoir conditions for the measurement of absolute permeability and true effective porosity of unconsolidated formations.
2. Permeability results indicate that absolute permeability of unconsolidated sand in its native state varies extensively with its shale and clay content. On the other hand, the arrangement of the particles and the degree of packing had little effect on absolute permeability.
3. Attempts were made to arrive at some correlations from the quantitative interpretation of electic logs and core analyses results to predict oil and water saturations. Due to the lack of formation resistivity factor data no reasonable correlations were obtained.
4. The presence of even small quantity of free water in the crude oil sample gave erroneous viscosities with the Rolling-ball viscometer.
5. The observed viscosities of dead crude oil did not compare favourably with other correlations. It is, thus, concluded that viscosity of dead crude oil in

the lower API range has no concrete relation with its density.

6. Appreciable decreases in viscosity were obtained with the first 30 cubic feet of gas in solution. The variation in viscosity with gas in solution compared favourably with Beal's correlation.
7. It was not possible to accurately define saturation pressure from pressure-volume relationship plot for this heavy crude oil. This was mainly attributed to extremely slow and different rate at which the dissolved gas came out of solution.

## REFERENCES

1. Core Laboratories Inc., "Summary of Core Analysis Procedures", Dellas Texas.

2. Elmdahl, B. A., "The Fundamental Principles of Core Analysis and Their Application to Gulf Coast Formations", AIME Technical Paper 588-G, Presented at Formation Evaluation Symposium, University of Houston, October 27-28, 1955.

3. Heid, J. G., McMahn, I. J., Nielson, R. F., and Yuster, S. L., "Study of the Permeability of Rocks to Homogeneous Fluids", API Drilling and Production Practices, 1950, Page 230.

4. Fettke, C. R., "Core Studies of the Second Sand of the Venango Group from Oil City, Pa.", AIME Trans. 1926, 219-233.

5. Elmdahl, B. A., "Core Analysis of Wicox Sands", World Oil, June 1952.

6. Cardwell, W. T., and Parsons, R. L., "Average Permeability of Hetrogeneous Oil Sands", AIME Technical Publication 1852, 1945.

7. Hubbard, R. M., and Brown, G. G., "The Rolling-ball Viscometer", University of Michigan, Ann Arbor, Michigan.

8. Hicott, C. R., and Backley, S. E., "Measurements of the viscosities of Oils Under Reservoir Conditions", New York Meeting, February, 1940.

9. Winn, R. H., "The Fundamentals of Quantitative Analysis of Electric Logs", Symposium on Formation Evaluation, AIME, October, 1955.

10. Archie, G. E., "The Electrical Resistivity Log as an Aid in Determining Some Reservoir Characterstics", AIME Technical Publication 1442.

11. Core Analysis, "Co-ordinated Program with Well Logging for Characterization of San Migual Sandstone",

( Technical Art. ) J. P. T., May, 1957, 425.

12. Wyllie, M. R. J., "Formation Factors of Unconsolidated Porous Media, Influence of Particle Shape and Effect of Cementaton", Trans. AIME 1953.

13. Botset, H. G., and Muskat, M., "Effects of Pressure Reduction Upon Saturation", AIME Trans. (1939) 172, Vol. 132.

14. Brown, J. S., "Formation Evaluation in Heavy Oil Sands", Heavy Oil Seminar, The Petroleum Society of C. I. M., Calgary, May 8, 1965.

15. Monk, G. D. "Analytical Study of Some Factors Affecting the Permeability and Porosity of Unconsolidated Sands", University of Chicago, M. S. Thesis, Geology (1940).

16. Tickell, G. G., and Hiatt, W. H.,"Effect of Angularity of Grain on Porosity and Permeability of Unconsolidated Sands", Bulletin American Association of Petroleum Geologist, (1939) 22, 1252 & 1279.

17. Hiatt, W. N., "A Study of the Permeabilities of Unconsolidated Sands", Engineers Thesis, Standford University (1938).

18. Craton, L. C. and Frazer, H. J., "Systametic Packing of Spheres", J. Geol. Vol. XLIII, 1955, Pp. 785-909.

19. Rockwood, S. H., "Analysis of Unconsolidated or Loosely Consolidated Core Samples", API Drilling and Production Practices 1948, 187.

20. Muskat, M., "Physical Principles of Oil Production", McGraw-Hill Book Company Inc., New York, 1949.

21. Francher, G. H., Lewis, J. A., and Barnes, M. B., " Some Physical Characterstics of Oil Sands", Penn. State College Mineral Industries Experimental Station Bulletin. 12, 1933, Pp.65.

22. Standing, M. R. and Katz, D. L., "Density of Crude Oils Saturated with Natural Gas", Trans. AIME

1942, Pp. 159.

23. Beal, C., "Viscosity of Air, Water, Natural Gas, Crude Oils and its Associated Gases at Oil Field Temperatures and Pressures", AIME Tech. Paper 2018 (1946)

24. Johnston, N., and Sherborne, J. E., "Permeability as Related to Productivity Index", API Drilling and Production Practices (1943) 68-69.

25. Trostel, E. G., "Production Gas-Oil Ratio as a Function of the Distribution of Hydrocarbons in the Underground Reservoir", Master's Thesis U. S. C., 1940.

# APPENDIX

T A B L E NO. 1

CORE ANALYSIS RESULTS
CORE FROM ABERFELDY POOL

| Sample No. | Mid Point of Sample | Representative of Feet | Permeability Millidarcies $K_H$ | Porosity Percent $\phi$ | Oil Saturation Percent $S_O$ | Water Saturation Percent $S_W$ | General Description |
|---|---|---|---|---|---|---|---|
| 1 | 1711.2 | 1710.0 - 1712.4 | - | - | - | - | - |
| 2 | 1712.9 | 1712.4 - 1713.4 | 305 | 39.9 | 71.0 | 8.0 | VF silty loose sand interbedded with shale, dark oil stains. |
| 3 | 1713.9 | 1713.4 - 1714.4 | 498 | 36.5 | 53.5 | 9.0 | " |
| 4 | 1714.7 | 1714.4 - 1715.0 | 146 | 36.7 | 47.2 | 15.7 | " |
| 5 | 1715.4 | 1715.0 - 1715.8 | - | 33.8 | 62.3 | 17.3 | VF silty loose sand interbedded with shale, traces of clay and silt. |
| 6 | 1716.2 | 1715.8 - 1716.6 | - | 37.4 | 49.3 | 15.4 | " |
| 7 | 1716.9 | 1716.6 - 1717.2 | - | 35.0 | 45.0 | Trace | VF silty loose sand, oil stains. |
| 8 | 1717.4 | 1717.2 - 1717.6 | 140 | - | - | - | Consolidated sandstone. |
| 9 | 1718.0 | 1717.6 - 1718.4 | - | - | - | - | Consolidated sandstone interbedded with shale. |
| 10 | 1718.8 | 1718.4 - 1719.2 | 100 | 33.8 | 70.0 | 20.3 | Five grain sand with silt on top. |
| 11 | 1719.6 | 1719.2 - 1720.0 | 1760 | - | - | - | Good unconsolidated sand. Shale near bottom. |

cont'd.

TABLE NO. 1 cont'd.

| Sample No. | Mid Point of Sample | Representative of Feet | Permeability Millidarcies $K_H$ | Porosity Percent $\phi$ | Oil Saturation Percent $S_O$ | Water Saturation Percent $S_W$ | General Description |
|---|---|---|---|---|---|---|---|
| 12 | 1720.4 | 1720.0 - 1720.8 | 3300 | 35.6 | 24.0 | 36.0 | Good unconsolidated sand. Shale near bottom. |
| 13 | 1721.2 | 1720.8 - 1721.6 | - | - | 20.0 | 37.0 | Fine silty loose packed sand interbedded with numerous shale breaks. Light oil stains. |
| 14 | 1722.0 | 1721.6 - 1722.4 | 855 | 35.7 | 45.0 | Trace | Fine silty loose packed sand, shale lense on top. Light oil stains. |
| 15 | 1723.2 | 1722.4 - 1724.0 | - | - | - | - | Fragile five grain sand interbedded with shale and silt. No oil stains. |
| 16 | 1724.5 | 1724.0 - 1725.0 | 23 | 21.3 | 88.5 | Trace | Interbedded shale, clay and Vf grain tight packed sand, dark oil stains. |
| 17 | 1725.25 | 1725.0 - 1725.5 | 1000 | 30.6 | 37.3 | 3.2 | VF grain silty loose packed sand with numerous shale breaks, dark oil stains. |
| 18 | 1725.75 | 1725.5 - 1726.0 | 800 | 28.1 | 50.0 | 3.5 | " |
| 19 | 1726.25 | 1726.0 - 1726.5 | 514 | 34.4 | 51.0 | 5.8 | " |
| 20 | 1726.75 | 1726.5 - 1727.0 | 406 | 37.5 | 51.0 | 1.7 | " |
| 21 | 1727.25 | 1727.0 - 1727.5 | 1008 | 34.6 | 30.0 | 2.0 | " |

cont'd.

TABLE NO. 1 cont'd.

| Sample No. | Mid Point of Sample | Representative of Feet | Permeability Millidarcies $K_H$ | Porosity Percent $\emptyset$ | Oil Saturation Percent $S_O$ | Water Saturation Percent $S_W$ | General Description |
|---|---|---|---|---|---|---|---|
| 22 | 1727.75 | 1727.5 - 1728.0 | 1051 | 38.4 | 36.0 | 1.0 | Vf grain silty loose packed sand with numerous shale breaks, dark oil stains. |
| 23 | 1728.25 | 1728.0 - 1728.5 | 367 | 27.5 | 32.0 | 11.9 | " |
| 24 | 1728.75 | 1728.5 - 1729.0 | 273 | 32.1 | 59.0 | 4.1 | " |
| 25 | 1729.25 | 1729.0 - 1730.0 | 671 | 35.0 | 17.2 | 1.9 | " |

Nomenclature

Vf - very fine

TABLE NO. 2

CORE ANALYSIS RESULTS
CORE FROM LONE ROCK POOL

| Sample No. | Mid Point of Sample | Representative of Feet | Permeability Millidarcies $K_H$ | Porosity Percent $\emptyset$ | Oil Saturation Percent $S_O$ | Water Saturation Percent $S_W$ | General Description |
|---|---|---|---|---|---|---|---|
| 1 | 1975.5 | 1975.0 - 1976.0 | - | 40.1 | 42.4 | 57.3 | VF silty loose sand, dark oil stains, highly oil saturated. |
| 2 | 1976.5 | 1976.0 - 1977.0 | 106 | 39.1 | 40.3 | 59.7 | " |
| 3 | 1977.5 | 1977.0 - 1978.0 | 195 | 36.5 | 59.4 | 40.6 | " |
| 4 | 1978.5 | 1978.0 - 1979.0 | 90 | 38.1 | 58.0 | 42.0 | " |
| 5 | 1979.5 | 1979.0 - 1980.0 | 51 | 40.0 | 52.6 | 47.4 | VF silty, tight packed sand, dark oil stains, oil saturated. |
| 6 | 1980.5 | 1980.0 - 1981.0 | - | 37.9 | 57.5 | 42.2 | VF silty, loose sand, dark oil stains, highly oil saturated. |
| 7 | 1981.5 | 1981.0 - 1982.0 | 111 | 39.0 | 44.4 | 53.6 | " |
| 8 | 1982.5 | 1982.0 - 1983.0 | 170 | 38.3 | 59.6 | 25.5 | " |
| 9 | 1983.5 | 1983.0 - 1984.0 | 227 | 36.0 | 61.1 | 15.5 | VF silty sand, dark oil stains, highly oil saturated. Top half loose packed, bottom half tight packed with coloured fragile shale. |
| 10 | 1984.5 | 1984.0 - 1985.0 | 409 | 36.0 | 70.7 | 19.1 | Fine silty tight packed sand, dark oil stains, highly oil saturated. |

cont'd.

TABLE NO. 2 cont'd.

| Sample No. | Mid Point of Sample | Representative of Feet | Permeability Millidarcies $K_H$ | Porosity Percent $\emptyset$ | Oil Saturation Percent $S_O$ | Water Saturation Percent $S_W$ | General Description |
|---|---|---|---|---|---|---|---|
| 11 | 1985.5 | 1985.0 - 1986.0 | 0.02 | 1.7 | 17.6 | 82.3 | VF grain consolidated sandstone or siltstone. |
| 12 | 1986.5 | 1986.0 - 1987.0 | - | - | - | - | " |
| 13 | 1987.5 | 1987.0 - 1988.0 | - | - | - | - | " |
| 14 | 1988.5 | 1988.0 - 1989.0 | - | - | - | - | " |
| 15 | 1989.5 | 1989.0 - 1990.0 | - | - | - | - | " |
| 16 | 1990.5 | 1990.0 - 1991.0 | 0.06 | 2.1 | 23.8 | 76.3 | " |
| 17 | 1991.5 | 1991.0 - 1992.0 | - | - | - | - | " |
| 18 | 1992.5 | 1992.0 - 1993.0 | - | 20.0 | 57.0 | 43.0 | Fine grain semiconsolidated sand, light oil stains, low oil saturation, interbedded shale. |
| 19 | 1993.5 | 1993.0 - 1994.0 | - | 19.8 | 29.6 | 62.5 | " |
| 20 | 1994.5 | 1994.0 - 1995.0 | - | 30.0 | 50.5 | 24.0 | " |
| 21 | 1995.5 | 1995.0 - 1996.0 | - | 32.4 | 39.2 | 39.8 | " |
| 22 | 1996.5 | 1996.0 - 1997.0 | - | 30.9 | 30.4 | 62.3 | " |
| 23 | 1997.5 | 1997.0 - 1998.0 | - | 22.6 | 62.5 | 37.5 | " |
| 24 | 1998.5 | 1998.0 - 1999.0 | - | 23.9 | 41.8 | 52.3 | " |
| 25 | 1999.5 | 1999.0 - 2000.0 | - | 23.6 | 56.4 | 26.9 | " |

cont'd.

TABLE NO. 2 cont'd.

| Sample No. | Mid Point of Sample | Representative of Feet | Permeability Millidarcies $K_H$ | Porosity Percent Ø | Oil Saturation Percent $S_O$ | Water Saturation Percent $S_W$ | General Description |
|---|---|---|---|---|---|---|---|
| 26 | 2000.5 | 2000.0 - 2001.0 | - | 23.6 | 33.5 | 56.8 | Fine grain semiconsolidated sand, light oil stains, low oil saturation, interbedded shale. |
| 27 | 2001.5 | 2001.0 - 2002.0 | - | 31.5 | 35.3 | 55.1 | " |
| 28 | 2002.5 | 2002.0 - 2003.0 | - | 18.5 | 25.8 | 67.5 | " |
| 29 | 2003.5 | 2003.0 - 2004.0 | - | 21.9 | 30.0 | 64.9 | " |
| 30 | 2004.5 | 2004.0 - 2005.0 | - | 17.7 | 90.1 | 9.9 | " |
| 31 | 2005.5 | 2005.0 - 2006.0 | - | 25.6 | 20.3 | 77.3 | " |
| 32 | 2006.5 | 2006.0 - 2007.0 | - | 22.9 | 51.1 | 48.9 | " |
| 33 | 2007.5 | 2007.0 - 2008.0 | - | 31.6 | 27.4 | 52.4 | " |
| 34 | 2008.5 | 2008.0 - 2009.0 | 108 | 22.9 | 55.1 | 40.0 | Fine silty tight packed sand, light oil stains, bottom half black hard shale. |
| 35 | 2009.5 | 2009.0 - 2010.0 | 375 | 26.9 | 36.1 | 47.3 | VF silty loose packed sand. Light oil stains. Bottom 4 inches light colored shale. |
| 36 | 2010.5 | 2010.0 - 2011.0 | - | 31.0 | 64.5 | 35.5 | " |
| 37 | 2011.5 | 2011.0 - 2012.0 | 1684 | 36.0 | 60.7 | 11.8 | VF grain silty loose packed sand. Light oil stains. |

cont'd.

TABLE NO. 2 cont'd.

| Sample No. | Mid Point of Sample | Representative of Feet | Permeability Millidarcies $K_H$ | Porosity Percent Ø | Oil Saturation Percent $S_O$ | Water Saturation Percent $S_W$ | General Description |
|---|---|---|---|---|---|---|---|
| 38 | 2012.5 | 2012.0 - 2013.0 | 745 | 37.3 | 62.2 | 7.9 | VF grain silty loose packed sand. Light oil stains, with few shale breaks. |
| 39 | 2013.5 | 2013.0 - 2014.0 | 602 | 32.7 | 64.0 | 13.0 | VF silty tight packed fragile sand, interbedded with thin strips of shale, light oil stains. |
| 40 | 2014.5 | 2014.0 - 2015.0 | 771 | 39.2 | 58.1 | 1.67 | " |
| 41 | 2015.5 | 2015.0 - 2016.0 | - | 32.6 | 70.8 | 26.5 | " |
| 42 | 2016.5 | 2016.0 - 2017.0 | 1478 | 35.9 | 70.0 | 8.2 | VF grain silty loose sand, dark oil stains, few thin strips of fragile shale. |
| 43 | 2017.5 | 2017.0 - 2018.0 | 840 | 34.3 | 66.8 | 15.2 | " |
| 44 | 2018.5 | 2018.0 - 2019.0 | 566 | 32.7 | 36.7 | 22.0 | " |
| 45 | 2019.5 | 2019.0 - 2020.0 | 759 | 34.3 | 64.1 | 19.1 | " |
| 46 | 2020.5 | 2020.0 - 2021.0 | - | 35.8 | 64.5 | 33.5 | " |
| 47 | 2021.5 | 2021.0 - 2022.0 | 270 | 34.3 | 82.2 | 17.8 | Fine silty tight packed sand, light oil stains, interbedded with thick layers of light coloured fragile shale. |
| 48 | 2022.5 | 2022.0 - 2023.0 | 498 | 34.3 | 63.8 | 26.7 | " |

cont'd.

TABLE NO. 2 cont'd.

| Sample No. | Mid Point of Sample | Representative of Feet | Permeability Millidarcies $K_H$ | Porosity Percent $\emptyset$ | Oil Saturation Percent $S_O$ | Water Saturation Percent $S_W$ | General Description |
|---|---|---|---|---|---|---|---|
| 49 | 2023.5 | 2023.0 - 2024.0 | - | - | - | - | Light coloured fragile shale. |
| 50 | 2024.5 | 2024.0 - 2025.0 | - | - | - | - | " |
| 51 | 2025.5 | 2025.0 - 2026.0 | - | 30.3 | 53.5 | 33.0 | Fine silty loose sand inter-bedded with light coloured shale. |
| 52 | 2026.5 | 2026.0 - 2027.0 | 412 | 31.0 | - | - | " |
| 53 | 2027.5 | 2027.0 - 2028.0 | - | - | - | - | Light coloured fragile shale. |
| 54 | 2028.5 | 2028.0 - 2029.0 | - | 30.1 | 32.4 | 34.4 | Fine silty loose sand inter-bedded with light coloured shale. |
| 55 | 2029.5 | 2029.0 - 2030.0 | - | - | - | - | Light coloured fragile shale. |
| 56 | 2030.5 | 2030.0 - 2031.0 | - | 28.6 | 17.1 | 80.4 | Fine silty loose sand, inter-bedded with light coloured shale. |

Nomenclature

VF - very fine

TABLE NO. 1 cont'd.

| Sample No. | Mid Point of Sample | Representative of Feet | Permeability Millidarcies $K_H$ | Porosity Percent $\emptyset$ | Oil Saturation Percent $S_O$ | Water Saturation Percent $S_W$ | General Description |
|---|---|---|---|---|---|---|---|
| 22 | 1727.75 | 1727.5 - 1728.0 | 1051 | 38.4 | 36.0 | 1.0 | Vf grain silty loose packed sand with numerous shale breaks, dark oil stains. |
| 23 | 1728.25 | 1728.0 - 1728.5 | 367 | 27.5 | 32.0 | 11.9 | " |
| 24 | 1728.75 | 1728.5 - 1729.0 | 273 | 32.1 | 59.0 | 4.1 | " |
| 25 | 1729.25 | 1729.0 - 1730.0 | 671 | 35.0 | 17.2 | 1.9 | " |

Nomenclature

Vf - very fine

TABLE 3.

WEIGHTED AVERAGE ROCK PROPERTIES FOR VARIOUS ZONES

ABERFELDY POOL

| | REPRESENTATIVE DEPTH INTERVAL (FT) | WEIGHTED AVG. K (md) | WEIGHTED AVG. Ø (%) | WEIGHTED AVG. So (%) | WEIGHTED AVG. Sw (%) | GENERAL DESCRIPTION |
|---|---|---|---|---|---|---|
| ZONE A | 1695 - 1700 | - | - | - | - | Core sample not available. |
| ZONE B | 1702 - 1703 | - | - | - | - | " " " " |
| ZONE C | 1705 - 1707 | - | - | - | - | " " " " |
| ZONE D | 1710 - 1718 | 228 | 34.60 | 56.50 | 11.10 | Very fine grain unconsolidated sand with consolidated sandstone and siltstone plus considerable amount of shale and shale breaks. |
| ZONE E | 1718 - 1722 | 1800 | 35.80 | 30.30 | 34.20 | Very fine grain unconsolidated sand with very little silt and clay. |
| ZONE F | 1722 - 1725 | 23 | 21.30 | - | 88.50 | Very little sand. Mostly silt, shale and clay. |
| ZONE G | 1725 - 1728 | 800 | 33.90 | 42.60 | 2.37 | Very fine grain unconsolidated sand with very little dark coloured shale breaks. |
| ZONE H | 1728 - 1733 | 390 | 33.80 | 38.30 | 4.90 | Very fine grain silty unconsolidated sand with shale and clay. |
| ZONE I | 1733 - 1738 | - | - | - | - | Core sample not available. |

TABLE 4.

WEIGHTED AVERAGE ROCK PROPERTIES FOR VARIOUS ZONES

LONEROCK POOL

| | REPRESENTATIVE DEPTH INTERVAL (FT) | WEIGHTED AVG. K (md) | WEIGHTED AVG. Ø (%) | WEIGHTED AVG. So (%) | WEIGHTED AVG. Sw (%) | GENERAL DESCRIPTION |
|---|---|---|---|---|---|---|
| ZONE A | 1968 - 1980 | 170 | 38.10 | 54.60 | 40.30 | Very fine silty unconsolidated sand with clay particles. |
| ZONE B | 1980 - 1987 | 0.05 | 2.0 | 20.0 | 78.30 | Consolidated siltstone. |
| ZONE C | 1987 - 2003 | | 27.50 | 42.60 | 48.80 | Semi consolidated very fine siltstone. |
| ZONE D | 2003 - 2006 | 240 | 23.60 | 51.90 | 40.90 | Very fine grain unconsolidated silty sand. Tight packed with shale and clay. |
| ZONE E | 2006 - 2012 | 1056 | 36.20 | 64.30 | 8.50 | Very fine grain unconsolidated sand. |
| ZONE F | 2012 - 2015 | 722 | 34.30 | 58.00 | 18.80 | Very fine grain unconsolidated silty sand. Little amount of shale and clay. |
| ZONE G | 2015 - 2019 | 384 | 34.30 | 73.00 | 22.30 | Very fine grain unconsolidated silty sand with strips of mud and light coloured fragile shale. |
| ZONE H | 2019 - 2024 | - | 30.40 | 43.50 | 33.70 | Light coloured fragile shale with few thin strips of fine unconsolidated sand. |
| ZONE I | 2024 - 2030 | - | 28.60 | 17.1 | 80.1 | Light coloured fragile shale with few thin strips of wet unconsolidated sand. |

TABLE NO. 5(A)

TYLER SIEVE ANALYSIS

SAMPLE NO. 6

| SCREEN MESH | SCREEN SIZE INCHES | WEIGHT RETAINED GRAMS | WEIGHT RETAINED PERCENT | CUMULATIVE WEIGHT RETAINED PERCENT | CUMULATIVE WEIGHT THROUGH PERCENT |
|---|---|---|---|---|---|
| 60 | 0.0097 | 0.7 | 1.45 | 1.45 | 98.55 |
| 80 | 0.0069 | 8.6 | 17.84 | 19.29 | 80.71 |
| 100 | 0.0058 | 15.5 | 32.16 | 51.45 | 48.55 |
| 120 | 0.0049 | 7.4 | 15.35 | 66.80 | 33.20 |
| 140 | 0.0041 | 6.3 | 13.07 | 79.87 | 20.13 |
| 200 | 0.0029 | 4.4 | 9.13 | 89.00 | 11.00 |
| 200+ | | 5.3 | 11.00 | 100.00 | 0.00 |
| TOTAL WEIGHT | | 48.2 | | | |

TABLE NO. 5(B)

TYLER SIEVE ANALYSIS

SAMPLE NO. 3

| SCREEN MESH | SCREEN SIZE INCHES | WEIGHT RETAINED GRAMS | WEIGHT RETAINED PERCENT | CUMULATIVE WEIGHT RETAINED PERCENT | CUMULATIVE WEIGHT THROUGH PERCENT |
|---|---|---|---|---|---|
| 60 | 0.0097 | 16.0 | 31.60 | 31.60 | 68.40 |
| 80 | 0.0069 | 0.7 | 1.38 | 32.98 | 67.02 |
| 100 | 0.0058 | 1.0 | 1.98 | 34.96 | 65.04 |
| 120 | 0.0049 | 0.6 | 1.19 | 36.15 | 63.85 |
| 140 | 0.0041 | 1.4 | 2.77 | 38.92 | 61.08 |
| 200 | 0.0029 | 0.5 | 0.99 | 39.91 | 60.09 |
| 200+ | | 30.4 | 60.10 | 100.00 | 0.00 |
| TOTAL WEIGHT | | 50.6 | | | |

TABLE NO. 5(C)

TYLER SIEVE ANALYSIS

SAMPLE NO. 12

| SCREEN MESH | SCREEN SIZE INCHES | WEIGHT RETAINED GRAMS | WEIGHT RETAINED PERCENT | CUMULATIVE WEIGHT RETAINED PERCENT | CUMULATIVE WEIGHT THROUGH PERCENT |
|---|---|---|---|---|---|
| 60 | 0.0097 | 4.7 | 9.57 | 9.57 | 90.43 |
| 80 | 0.0069 | 1.1 | 2.21 | 11.80 | 88.20 |
| 100 | 0.0058 | 1.0 | 2.04 | 13.84 | 68.17 |
| 120 | 0.0049 | 1.0 | 2.04 | 15.88 | 84.12 |
| 140 | 0.0041 | 1.7 | 3.47 | 19.35 | 80.65 |
| 200 | 0.0029 | 6.0 | 12.25 | 31.60 | 68.40 |
| 200+ | | 33.5 | 68.40 | 10.00 | 0.00 |
| TOTAL WEIGHT | | 49.0 | | | |

TABLE NO. 5(D)

TYLER SIEVE ANALYSIS

SAMPLE NO. 21

| SCREEN MESH | SCREEN SIZE INCHES | WEIGHT RETAINED GRAMS | WEIGHT RETAINED PERCENT | CUMULATIVE WEIGHT RETAINED PERCENT | CUMULATIVE WEIGHT THROUGH PERCENT |
|---|---|---|---|---|---|
| 60 | 0.0097 | 11.2 | 17.30 | 17.30 | 82.70 |
| 80 | 0.0069 | 1.2 | 1.85 | 19.15 | 80.85 |
| 100 | 0.0058 | 1.7 | 2.62 | 21.77 | 78.23 |
| 120 | 0.0049 | 8.5 | 13.11 | 34.88 | 65.12 |
| 140 | 0.0041 | 9.5 | 14.67 | 49.55 | 50.45 |
| 200 | 0.0029 | 13.6 | 21.00 | 70.55 | 29.45 |
| 200+ | | 19.1 | 29.45 | 100.00 | 0.00 |
| TOTAL WEIGHT | | 44.8 | | | |

TABLE NO. 6

VISCOSITY READINGS AT 75 $^{o}$F FOR DIFFERENT SAMPLES

| DEAD CRUDE OIL | | SAMPLE WITH 5 SCF/STB | | SAMPLE WITH 10 SCF/STB | |
|---|---|---|---|---|---|
| PRESSURE PSI | VISCOSITY CPS | PRESSURE PSI | VISCOSITY CPS | PRESSURE PSI | VISCOSITY CPS |
| 104 | 760 | 230 | 720 | 310 | 660 |
| 199 | 775 | 403 | 730 | 395 | 670 |
| 299 | 785 | 500 | 740 | 500 | 685 |
| 397 | 800 | 603 | 755 | 598 | 700 |
| 498 | 815 | 700 | 770 | 697 | 715 |
| 598 | 825 | 803 | 785 | 804 | 725 |
| 700 | 835 | 898 | 805 | 895 | 740 |
| 806 | 850 | 798 | 785 | 810 | 730 |
| 800 | 845 | 752 | 775 | 705 | 710 |
| 695 | 835 | 700 | 770 | 604 | 695 |
| 502 | 815 | 656 | 765 | 490 | 685 |
| 400 | 800 | 500 | 755 | 405 | 670 |
| 299 | 785 | 405 | 730 | 330 | 660 |
| 205 | 775 | 240 | 720 | 410 | 670 |

TABLE NO. 6 Cont'd.

| SAMPLE WITH 15 SCF/STB | | SAMPLE WITH 25 SCF/STB | | SAMPLE WITH 30 SCF/STB | |
|---|---|---|---|---|---|
| PRESSURE PSI | VISCOSITY CPS | PRESSURE PSI | VISCOSITY CPS | PRESSURE PSI | VISCOSITY CPS |
| 200 | 595 | 970 | 630 | 390 | 555 |
| 305 | 610 | 888 | 615 | 488 | 565 |
| 406 | 620 | 798 | 605 | 590 | 575 |
| 500 | 635 | 693 | 595 | 690 | 580 |
| 600 | 645 | 596 | 580 | 794 | 595 |
| 696 | 660 | 510 | 570 | 893 | 605 |
| 800 | 675 | 398 | 560 | 946 | 615 |
| 900 | 690 | 302 | 550 | 853 | 605 |
| 798 | 680 | 406 | 565 | 754 | 595 |
| 706 | 665 | 500 | 575 | 652 | 580 |
| 604 | 650 | 602 | 580 | 562 | 570 |
| 504 | 635 | 703 | 595 | 453 | 565 |
| 400 | 620 | 806 | 605 | 352 | 550 |
| 300 | 610 | 970 | 630 | 450 | 565 |

TABLE NO. (7A)

PRESSURE - VOLUME RELATIONSHIP FOR DETERMINATION OF SATURATION PRESSURE AT 80° F.

Sample with 25 cu. ft. of gas in solution.

| PRESSURE PSI | PUMP READING | VOLUME c.c. | DATE |
|---|---|---|---|
| 1025 | 245.712 | 50.000 | 2.2.65 |
| 896 | 245.603 | 50.109 | 3.2.65 |
| 805 | 245.521 | 50.191 | 4.2.65 |
| 720 | 245.429 | 50.293 | 5.2.65 |
| 606 | 245.320 | 50.392 | 5.2.65 |
| 523 | 245.220 | 50.492 | 6.2.65 |
| 415 | 245.090 | 50.622 | 6.2.65 |
| 356 | 245.001 | 50.711 | 7.2.65 |
| 297 | 244.915 | 50.797 | 7.2.65 |
| 256 | 244.860 | 50.852 | 8.2.65 |
| 200 | 244.160 | 51.552 | 10.2.65 |
| 170 | 243.158 | 52.554 | 19.2.65 |
| 125 | 240.402 | 55.310 | 29.2.65 |
| 110 | 238.140 | 57.570 | 10.3.65 |

TABLE NO. (7B)

Sample with 10 cu. ft. of gas in solution.

| PRESSURE PSI | PUMP READING | VOLUME c.c. | DATE |
|---|---|---|---|
| 1004 | 246.673 | 50.000 | 6.3.65 |
| 907 | 246.577 | 50.096 | 7.3.65 |
| 808 | 246.484 | 50.189 | 7.3.65 |
| 710 | 246.381 | 50.292 | 8.3.65 |
| 620 | 246.280 | 50.393 | 8.3.65 |
| 505 | 246.155 | 50.518 | 9.3.65 |
| 420 | 246.050 | 50.623 | 9.3.65 |
| 305 | 245.920 | 50.753 | 10.3.65 |
| 200 | 245.812 | 50.861 | 10.3.65 |
| 150 | 245.761 | 50.912 | 19.3.65 |
| 125 | 245.730 | 50.943 | 23.3.65 |
| 100 | 245.463 | 51.210 | 25.3.65 |
| 60 | 244.993 | 51.680 | 28.3.65 |
| 35 | 243.663 | 53.010 | 29.3.65 |

TABLE NO. (7C)

Sample with 30 cu. ft. of gas in solution.

| PRESSURE PSI | PUMP READING | VOLUME c.c. | DATE |
|---|---|---|---|
| 999 | 246.922 | 50.00 | 20.12.64 |
| 902 | 246.832 | 50.090 | 21.12.64 |
| 804 | 246.748 | 50.174 | 22.12.64 |
| 712 | 246.658 | 50.264 | 23.12.64 |
| 597 | 246.558 | 50.364 | 24.12.64 |
| 525 | 246.472 | 50.450 | 28.12.64 |
| 430 | 246.354 | 50.568 | 29.12.64 |
| 370 | 246.280 | 50.642 | 30.12.64 |
| 318 | 246.200 | 50.722 | 3. 1.65 |
| 251 | 245.672 | 51.250 | 15. 1.65 |
| 200 | 243.691 | 53.231 | 20. 1.65 |
| 175 | 241.622 | 55.300 | 25. 1.65 |
| 150 | 237.922 | 59.000 | 28. 1.65 |
| | | | 1. 2.65 |

## TABLE NO. 8

### CALIBRATION OF BENIDIX-LAB VISCOMETER.

Standard Range was calibrated for the range of 65 cps.xgms per cc. to 525 cps.x gms per cc. at 77.5° F.

| | |
|---|---|
| Zero Control | 8632 |
| Calibration control | 2129 |

Special Range was calibrated for the range of 525 cps.x gms per cc. to 1150 cps.x gms per cc. at 77.5° F.

| | |
|---|---|
| Zero Control | 8520 |
| Calibration Control | 2308 |